

6. The Ocean's Response to North Atlantic Oscillation Variability

Martin Visbeck

Department of Earth and Environmental Sciences
LDEO, Columbia University
RT9W, Palisades, NY 10964, USA
visbeck@ldeo.columbia.edu

Eric P. Chassignet

RSMAS/MPO
University of Miami, FL, USA

Ruth Curry

Physical Oceanography Department
Woods Hole Oceanographic Institution
Woods Hole, MA, USA

Tom Delworth

GFDL/NOAA
Princeton, NJ, USA

Bob Dickson

Center for Environment, Fisheries and Aquaculture Science
Lowestoft Laboratory, UK

Gerd Krahlmann

Lamont-Doherty Earth Observatory
Palisades, NY, USA

Abstract:

The North Atlantic Oscillation is the dominant mode of atmospheric variability in the North Atlantic Sector. Basin scale changes in the atmospheric forcing significantly affect the oceans' properties and circulation. Part of the ocean's response is local and rapid (surface temperature, mixed layer depth, upper ocean heat content, surface Ekman transport, sea ice cover). However, the geostrophically balanced large scale horizontal and overturning ocean circulation response can take several years to adjust to changes in the forcing. The delayed response is non-local in the sense that perturbations at the air sea interface will be communicated by waves and the mean circulation to other parts of the basin. A delayed and non-local response can potentially give rise to oscillatory behavior if there is significant feedback from the ocean to the atmosphere (see Czaja et al, this volume). We conjecture that on decadal and longer time scales, changes in the oceans' heat storage and heat transport should have an increasingly important impact on the climate. Finally, changes in the ocean circulation and distribution of heat and freshwater will also alter the ocean's ventilation rates and pathways. Thus we expect a change in the net uptake of gases (e.g. O₂, CO₂), altered nutrient balance, and changes in the dispersion of marine life (see Drinkwater et al., this volume, for a discussion on changes in the marine ecosystem). We begin by a short introduction and then review what is known about the oceans response to changes in the NAO induced forcing from combined theoretical, numerical experimentation and observational perspectives.

6.1 INTRODUCTION

More than two centuries ago, missionaries noticed that the interannual temperature fluctuations in wintertime air temperature across the North Atlantic ocean were out of phase between Greenland and Denmark [see Hurrell et al., this volume, and Thompson et al, this volume, for recent reviews]. In the early part of the twentieth century, Walker analyzed the spatial correlation patterns of seasonal weather and noticed a surface pressure correlation pattern within the Atlantic sector that he referred to as the "North Atlantic Oscillation" (NAO) [Walker and Bliss 1932]. In a seminal paper several decades later, Bjerknes discussed his views of air-sea interactions in the Atlantic, addressing "... causes of the variations in the surface temperature of the Atlantic Ocean from year to year and over longer periods" [Bjerknes 1964]. He interpreted the changes in ocean temperatures as partly due to radiative transfer and heat exchanges at the interface between oceans and atmosphere, and partly due to advective heat transport divergence as a result of varying ocean currents. Most of these fluxes depend directly on the strength of the wind, and Bjerknes refers to those large scale changes as years of "low-index" and "high-index". The associated pattern in sea level pressure was given the name the North Atlantic Oscillation [Wallace and Gutzler 1981; Stephenson et al., this volume; Jones et al., this volume]. The advent of global data sets and advances in theory and computer model simulations over the last decade have revitalized the interest in the NAO and its interaction with the ocean, sea ice and other parts of the climate system. Many of the early concepts have survived. However, the increased observational database, models and a more complete theory of ocean and atmospheric circulation have helped to sharpen our hypothesis and understanding. The NAO is now widely recognized as the most significant pattern of climate variability in the North Atlantic Sector and a strong competitor to ENSO in terms of global significance [e.g. Marshall et al. 2001b; Hurrell et al. 2001; Visbeck et al. 2001].

Here we examine the oceans response to changes in the atmospheric forcing associated with the NAO. The oceans large heat capacity (2.5 m of water contains as much thermal energy as the entire atmospheric column) makes it the 'flywheel' of the climate system. How does it change in response to NAO-induced forcing? If the ocean and atmosphere were tightly coupled to each other, one might question why consider only the ocean's response? However, outside of the deep tropics, most studies find that the ocean largely reacts to the high frequency changes of the atmospheric forcing and that its influence back to the atmosphere is weak on time scales shorter than a decade. Thus the emerging null hypothesis is one where the ocean merely responds to and integrates in time the atmospheric forcing anomalies in the spirit of the stochastic climate model of Hasselman [1976] and Frankignoul and Hasselman [1977]. Is it really true? Or does the ocean have more in stock than one could explain by a local response? We will give evidence for both local and remote responses, but we refer the reader to Czaja et al [this volume] for a comprehensive review of possible ocean-atmosphere coupling mechanisms [see also Czaja and Marshall 2001] in the context of the NAO.

In most of the following, we will focus on the winter season as the time of NAO forcing. As shown by Hurrell et al. [this volume], the NAO forcing is most active between November and April, at a time when the ocean mixed layers are deep and much of the ocean uptake of gases takes place. One can identify an NAO signature in the summer season, but it is weaker, less persistent and explains only a small fraction of the overall variance. We will define a 'typical' NAO perturbation using regression techniques and study the oceans response to it. Such NAO forcing patterns are quite robust between different methods, data sets, and decades. However, we caution that any attempts to identify 'normal' or 'standard' patterns of NAO behavior and the associated ocean response will necessarily be oversimplified. For example, a slight eastward shift of the NAO dipole pattern in certain winters of the late 1990s was enough to reverse a cooling and freshening trend in Labrador Sea Water that had persisted for decades despite a positive NAO

index. Hilmer and Jung [2000] suggest that the centers of maximum interannual variability in SLP associated with the NAO have been located further to the east since the late 1970s and dramatically changed the sea-ice response. Those observations, – i.e. that NAO-positive conditions can locally drive quite different ocean responses depending on the detailed configuration of the associated sea level pressure pattern, – offers a timely reminder of the limitations of using a simple 2-point pressure difference as our index of NAO behavior. It remains to be seen whether those shifts in the 'standard' NAO pattern are just further evidence of the chaotic nature of the atmospheric circulation –i.e. NAO noise– or are part of a more concerted trend in NAO behavior. In other words, both the detailed configuration of the NAO and the ocean's response to it can be expected to change.

First we revisit the observational evidence of NAO-related changes in the sea surface temperatures, and then discuss what is known about the air-sea fluxes that force them. The next two sections apply ocean circulation theory to provide an idea about NAO-induced ocean circulation changes. Those circulation changes can directly impact the ocean heat transport, which potentially could introduce non-local atmospheric feedback. The advection of the anomalies themselves by the mean circulation is of interest for the same reason. In subsection 5 and 6, we review the observational evidence of the modulation of ocean deep convection and changes in water mass composition with special emphasis on the recent trends. The last section reviews the sea-ice response to changes in NAO and we close with a brief summary and discussion.

6.2 OBSERVED SST RESPONSE PATTERN

The North Atlantic Oceans' surface temperature response to changes in the NAO index has been described carefully by the early work of Bjerknes [1962]. He compared individual winter seasons with a "high" and "low" index and found warmer temperatures between 30°N and 45°N in the western North Atlantic and cooler temperatures in the subpolar gyre region (north of 45°N). More recent studies [e.g. Cayan 1992a; Visbeck et al. 1998; Seager et al. 2000; Marshall et al. 2001a] correlated SST anomalies from the NCEP-NCAR reanalysis with the NAO index and reproduced a similar response pattern. However, the amplitudes seen in this case are somewhat lower (~ 0.5 °C for a strong NAO event) when compared to earlier maps based on individual years and smaller regions which exhibit differences of up to 2°C for a strong NAO event. As an example, we present, covariance and correlation between a 100 year long SST anomaly data set [Kaplan et al. 1997, 1998] and the NAO index [Hurrell 1995] (Figure 1). In addition to the Bjerknes North Atlantic SST dipole, a large third lobe in the northern tropical Atlantic is apparent. The latter plays an important role in tropical Atlantic Variability [e.g. Marshall et al 2001b] and can displace the location of large tropical precipitation within the ITCZ. This three lobe SST response pattern is often referred to as the "NAO SST tripole" pattern. It also appears as the second EOF when global SST anomalies are analyzed. Maximum correlation is 0.4 in the centers of action, and the maximum SST covariance with the NAO index is about 0.3°C at zero lag. Thus the NAO explains only 20-40% of the local winter season SST variance.

Lag correlation between SST and the NAO index are interesting since they contain information about the coupling between atmosphere and ocean. If a coherent SST pattern leads the NAO index and SST itself varies either slowly or predictably, one would be able to construct a statistical NAO prediction system (see Czaja et al. [this volume]; and Rodwell [this volume] for a discussion on predictability). However, if the ocean is merely responding to NAO related atmospheric forcing, one would then expect a strong asymmetry in the lag correlation, with weak correlation prior to an NAO event and more persistent correlation when the ocean lags the atmosphere. Lag correlation between the Kaplan SST data set and the NAO index from 1901-2000 shows that the largest correlation is at zero lag, with some limited ocean memory with lags

of up to 3 years in the Gulf Stream extension region (Figure 2). Watanabe and Kimoto [2000] remark that this persistence is longer than what would be expected from local damping due to air-sea interaction, which yields a decay scale of about 3 months [Frankignoul et al. 1998]. This is consistent with the so-called reemergence mechanism in which a shallow summer thermocline shields deeper temperature anomalies from the atmosphere, which then are reentrained in the following winter season [Alexander and Deser 1995]. However, the displacement of SST anomalies along the path of the mean ocean currents might suggest some role for ocean advection [Sutton and Allan 1997]. Only small regions of significant correlation where SST anomalies are leading NAO events were found here (Figure 2). Thus the observed NAO-SST relationship supports a strong and immediate response of the surface ocean, with limited evidence for multi-season persistence and little support for strong atmospheric response [Kushnir et al. 2002, see also Czaja et al., this volume, for an in depth discussion].

A similar three-lobe mode of SST variability within the Atlantic sector, with centers of action in the subpolar gyre, subtropical gyre, and northern equatorial region, has been found in a large number of observational, modeling, and theoretical studies of North Atlantic climate variability [e.g. Deser and Blackmon 1993; Kushnir 1994; Battisti et al. 1995; Luksch 1996; Delworth, 1996; Halliwell 1998; Seager et al. 2000; Grötzner et al. 1998; Selten et al. 1999; Xie and Tanimoto 1998]. In all cases, the ocean is responding to variable atmospheric forcing with a preferred spatial structure. However, there are considerable differences in opinion, and possible model sensitivity, with regard to mechanisms that cause changes in SST, in particular the relative role of air-sea heat fluxes versus momentum flux-induced changes in the ocean circulation and the role of ocean circulation in general.

For example, Battisti et al. [1995] and Seager et al. [2000] show that SST variability on interannual time scales over the Atlantic can be understood in terms of one-dimensional mixed layer processes, except in the region of the separated Gulf Stream / North Atlantic current where advection by ocean currents is hypothesized to be important.

While there is consensus on the fast (seasonal to interannual) response of the ocean to NAO forcing the decadal and long-term response is controversial. Kushnir [1994] shows that the decadal mode of SST variability is more of a hemispheric one sign response and thus different from the interannual tripolar SST pattern. Visbeck et al. [1998] and Krahnmann et al. [2001] argue that this is the expected response for low frequency NAO forcing and that on multi decadal time scales, the NAO-induced SST response switches from a dipolar pattern between the subpolar and subtropical gyre to one-sign monopole response. They propose that this is due to advection of anomalous temperatures by the Gulf Stream / North Atlantic Current system. Delworth and Greatbatch [2000] and Eden and Willebrand [2001] find a similar low frequency basin scale response. However, they attribute it to NAO-induced modulation in the upper ocean circulation as part of the Atlantic Ocean meridional overturning.

Thus care has to be taken when attributing a particular SST response pattern to the NAO since the ocean's dynamical response, which takes several years to be fully established, is non local and able to substantially alter the air-sea heat flux driven SST response pattern. In the following sections, we discuss in more detail several of the proposed mechanisms that cause the observed NAO-induced SST response.

6.3 AIR-SEA FLUX

The NAO involves a shift in atmospheric mass between the subtropics and the polar regions [e.g., Hurrell and van Loon 1997; Hurrell et al. 2001, Hurrell et al., this volume and Thompson et al,

this volume]. During the high index phase, the Icelandic (polar) low is anomalously low and the Azores (subtropical) high is anomalously high. Consequently the midlatitude surface westerly winds are strong, as are the easterly surface winds in the trade wind belt. The North Atlantic storm track is well developed and has a signature that extends from the U.S. east coast to the British Isles and Scandinavia. In the low index phase, both the Icelandic low and the Azores high are weak, the westerlies and trades are weaker. Fewer storms are found during that phase. Some have the tendency to move from the United States into the Labrador Sea region, while those that make it across the Atlantic move into southern Europe and the Mediterranean. Thus the NAO not only affects the strength but also the position of the maximum westerlies and storm frequency and intensity. Variations in the NAO index and associated wind fields imply strong changes in surface air-sea flux fields of heat, momentum, and water. These changes impact both the local thermodynamic response of the mixed layer and the large-scale circulation field. We continue to examine how each of these fluxes vary with the NAO, and their implications for the North Atlantic Ocean.

6.3.1 Momentum Flux

Figure 3 shows the correlation and covariance between the NAO index and the winter season averaged wind stress. High correlation is found in two bands, one centered at 60°N and the other at 30°N, each of which is about 15° wide. The NAO-induced changes in the wind stress are largest at 60°N; however, their relative magnitude compared to the mean wind stress is largest at the northern and southern boundaries of the west wind regime (65°N and 35°N). The overall pattern shows enhanced and northerly displaced westerlies north of 45°N, as well as slightly enhanced trade winds between 10°N and 30°N. Notice also the increased advection of cold Arctic air masses within the Labrador Sea and the western part of the Greenland Sea, as inferred from the covariance of wind stress. We agree with Marshall et al. [2001a], that the associated changes in the wind stress curl can be best understood as a meridional shift in the mean pattern rather than as a modulation of its strength.

6.3.2 Heat Flux

Changes in the local air-sea heat fluxes are a likely cause for the observed SST anomaly pattern. The heat flux can be divided into four components, the net short wave and long wave radiation and the sensible and latent heat flux anomalies. Variability in the net short wave radiation will depend on changes in cloudiness and the sea-ice albedo. Changes in the net long wave radiation are due to changes in the lower atmospheric temperature, cloudiness, or SST. Long wave radiation anomalies tend to damp SST anomalies. The sensible and latent heat fluxes depend on gradients between the lower atmosphere and the sea surface in temperature or water vapor pressure respectively. However, both heat fluxes depend strongly on the surface wind speed and thus are well correlated.

Cayan [1992a, 1992b] was the first to systematically examine the relationship between surface pressure anomalies, upper ocean temperature changes, and sensible and latent air-sea fluxes using the COADS (Comprehensive Ocean-Atmosphere Data Set) data set [Woodruff et al. 1987]. He used an EOF analysis based on monthly sea level pressure, SST tendency, and sensible and latent heat flux anomalies. In comparison, we show heat flux anomalies regressed on the NAO index, using the NCEP-NCAR winter season averaged (DJFM) anomalies (Figure 4). In the subpolar gyre, the largest flux anomalies are due to the sensible heat loss closely followed by evaporative heat loss. In the subtropical gyre, the flux anomalies are weaker and are dominated by evaporation. The sum is about 20-40 W m⁻² and is significantly lower than the monthly based analysis of Cayan [1992a], who found values of up to 100 W m⁻². The difference is largely due to the use of a winter season average anomalies in Figure 4. Seager et al. [2000] discuss the relative

importance of the local air-sea fluxes due to changes in wind speed versus changes in the advection of air masses. They find that equatorward of 40°N changes in wind speed are most important while poleward of 40°N both play an equal role. Variations in short wave radiative fluxes induced by changes in the cloud cover are approximately an order of magnitude smaller and are not shown. The response of the net long wave radiation is also small in the NCEP/NCAR reanalysis data set, but one might question how realistic cloud variability is represented in this model.

Finally, changes in the Ekman transport induced upper ocean heat transport divergences (see next section) are significant. Following Marshall et al [2001a] one can compute from the changes in wind stress a field of upper ocean Ekman transport anomalies. This NAO induced Ekman transport can be then multiplied by the mean upper ocean temperature and its divergence can be expressed as a pseudo surface heat flux (Figure 4c). This flux anomaly pattern is roughly similar to the sum of sensible and latent heat fluxes with values of up to 20 W m⁻² near the Gulf Stream/North Atlantic Current region east of 50°W. We have also estimated the contribution due to the mean surface Ekman transport divergence acting on the anomalous temperature gradient and found this term to be quite a bit smaller compared to other flux anomalies.

Can those air sea flux anomalies explain the observed SST anomalies? A 50 W m⁻² heat flux anomaly would warm a 100 m deep mixed layer by 1°C in about 100 days, which is of the same order as the observed interannual variations in SST. A more precise answer to this question would allow us to accept or refute the "null hypothesis" of the oceans response being merely a one dimensional integrator of air-sea fluxes (section 6.1). Unfortunately, one would need both, good observations of the upper ocean heat content (SST and mixed-layer depth, which is quite variable in the mean and interannually) as well as high quality observations of air-sea flux anomalies, neither of which is currently accurately enough to rule out a significant role of ocean dynamics. Model aided studies such as the one of Seager et al. [2000] still suffer from uncertainties in the air-sea flux formulation and have ignored the contribution of a variable depth mixed layer and thus can not provide final proof. However, let's consider a sustained NAO induced heat flux anomaly winter after winter. One would expect slowly growing SST anomalies, even if the heat flux anomalies are reduced on longer time scales. Thus one might suspect that on long time scales, changes in the ocean circulation and thus the changes in ocean heat transport divergence will balance the remaining long term air sea flux anomaly. On interannual time scales, however, the good spatial correspondence of the air-sea flux anomalies with the SST anomalies as well as their corresponding magnitude explains why the short term upper ocean temperature response can be rationalized in terms of a simple local mixed layer heat budget calculation [e.g. Battisti et al. 1995; Seager et al. 2000].

6.3.3 Water Flux

Much less is known about the balance between evaporation, which is proportional to the latent heat flux, and precipitation. Figure 5 shows the covariance of winter mean evaporation and precipitation with the NAO index. The changes in the position of the storm track and associated moisture transport result in a dipole pattern with enhanced rainfall over northern Europe and reduced precipitation from the Canary Islands toward the Mediterranean Sea [Hurrell, 1995]. Just like in the discussion of heat fluxes, we can consider the anomalous Ekman freshwater transport divergence as part of the net surface fresh water flux [Mignot, pers. comm. 2002]. The resulting pattern shows significant freshening along the North Atlantic Current as well as the East and West Greenland Currents. The largest fresh water loss is expected along the Labrador Current. Parts of the precipitation anomalies are canceled by evaporation, however, and the net fresh water exchange sign and pattern are dominated by both the precipitation and Ekman induced fresh water fluxes (Figure 5d). Little is known about basin scale changes in the surface

salinity field due to NAO forcing. However, decadal salinity variability in the North Atlantic region has been described as related to NAO forcing [Reverdin et al. 1997; 1999; Houghton and Visbeck, 2002].

6.3.4 Buoyancy Flux

Changes in the oceans' large scale surface density gradient can alter the strength and character of the basin scale meridional ocean overturning. The surface density flux depends on both the air-sea heat flux and the net fresh water flux, which can be combined into a buoyancy flux anomaly by multiplying them by the thermal and haline expansion coefficients, respectively (Figure 6). We find that the zonally averaged response is dominated by the heat flux contribution with maximum values of $1 \times 10^{-8} \text{ m}^2 \text{ s}^{-3}$. One of the important impacts of enhanced or reduced surface buoyancy flux is its impact on the maximum late winter mixed layer depth. In general one would expect an increase in late winter mixed-layer depth in the subpolar gyre and a reduction in mixed-layer depth in the subtropical gyre for a positive NAO index season. Khatiwala et al. [2002] and Marsh [2000] have calculated the implied variability in water mass transformation rates due to interannual changes in the surface buoyancy flux. In the Labrador Sea the production of Labrador Sea water was expected to have increased from its mean value of 2.7 Sv ($1 \text{ Sv} = 10^6 \text{ m}^3 \text{ s}^{-1}$) to 4 Sv during the high NAO period in the early 1990ies.

4. RESPONSE OF THE OCEAN CIRCULATION

Large changes in the strength and direction of the surface wind stress associated with the NAO will alter the momentum and buoyancy balance of the North Atlantic Ocean. Here we ask: What is the response of the ocean circulation to NAO induced changes in the surface forcing? Simplified ocean dynamics can provide us with some guidance regarding the expected ocean circulation response. We first treat the wind and buoyancy driven circulation separately, then review the observational evidence and finally summarize the more complex NAO response found in ocean general circulation models.

6.4.1 Response of the Wind Driven Ocean Circulation

Large scale anomalies of the surface wind stress field will alter the surface frictional balance and cause an immediate response of the upper wind driven circulation. The upper layer vertical integral of the horizontal flow, the Ekman transport (M_{ek}), is proportional to the wind stress anomaly (τ') divided by a reference density (ρ_0) and Coriolis parameter (f):

$$M_{ek} = (-\mathbf{k} \times \boldsymbol{\tau}') / (\rho_0 f),$$

with \mathbf{k} a unit vector in the vertical. The Ekman transport adjusts on short time scales (several days) and thus will be in phase with the seasonal NAO related forcing anomaly. Since the wind stress anomalies vary little in the zonal direction, we limit our discussion of the zonally averaged response. During a positive NAO index phase, we find poleward Ekman transport south of 40°N and equatorward Ekman transport north of 40°N (Figure 7). Note, as mentioned in the previous section, a changing Ekman transport also induces an upper ocean heat transport divergence [Marshall et al. 2001a] which consequently acts similar to air-sea fluxes of heat and freshwater.

The zonally integrated Ekman transport shows maximum southward advection of 3 Sv at 58°N and maximum northward surface flow at 30°N . Between those latitudes, the zonally averaged Ekman transport is convergent and must be balanced by downwelling below the surface layer. If we assume no net meridional transport, which is true in the Atlantic to about 1 Sv uncertainty,

then the zonally averaged mean surface transport (mean and anomaly) must be balanced by an equal and opposite flow below. Thus the zonally averaged surface Ekman transport contributes to the meridional overturning circulation stream function with a maximum below the Ekman layer at a depth $h_{ek} \sim 300\text{m}$. This Ekman part of the ocean meridional circulation's response to changes in the NAO forcing can be expressed as:

$$\Phi_{ek,max} = \int M_{ek} dx.$$

For a homogeneous ocean with small internal friction but significant bottom friction, the return flow will occur in the frictional bottom boundary layer. On the other hand, a strongly stratified ocean basin will allow for a geostrophically balanced shallower return flow. Note that in both scenarios, we expect rapid communication with the deeper ocean circulation. Figure 7 shows the Ekman induced zonally averaged overturning ($\Phi_{ek,max}$) expected for a positive NAO index phase. At 50°N , we expect the meridional overturning to be reduced by 1-2 Sv while at 30°N , the poleward surface transport should be enhanced by 1 Sv.

Changes in the Ekman transport divergence (Figure 7c,d) cause up/downwelling and thus perturb the large scale potential vorticity balance of the oceans gyre's. The adjustment towards a new balanced state is established by coastally trapped (boundary) waves, equatorial Kelvin waves, and long Rossby waves. While boundary and Kelvin waves have relatively fast phase speeds, the westward propagating long Rossby are much slower with decreasing phase speeds towards higher latitudes. The Rossby wave phase speed is also a function of the baroclinic mode with the higher vertical modes taking again much longer to adjust. The basin adjustment time scale is governed by the slowest component of the most energetic vertical mode and thus is expected to be on the order of a few years for the first baroclinic mode. The higher vertical modes take much longer to adjust (on the order of a decade or more).

A simple form of the steady state gyre response can be obtained by diagnosing the planetary potential vorticity balance for the depth averaged *Sverdrup* (M_{sv}) interior transport:

$$M_{sv} = \int (\nabla \times \tau') dx / (\rho_0 \beta) ,$$

where β denotes the change of the Coriolis parameter with latitude. (Note, that in particular in the northern North Atlantic the Sverdrup balance might not hold due to the importance of interaction between the deep density field and the complex topography.) We can evaluate this integral from the eastern boundary of the ocean to a point close to the western boundary to obtain an estimate for the expected changes in the western boundary current transport that balance the input of planetary vorticity by the anomalous wind stress. Figure 7d shows the anomalous equilibrium response of the North Atlantic Ocean and we expect changes of 5-8 Sv of the western boundary current transport which are consistent with similar estimates by Joyce et al. [2000]. The region of maximum change at 45°N is located between the two main gyres and thus has been dubbed the "intergyre gyre" [Marshall et al. 2001a]. The "intergyre gyre" refers to the anomalous circulation pattern that emerges when differencing the positive from the negative ocean gyre circulation (see also Figure 3d).

6.4.2 Response of the Buoyancy Driven Ocean Circulation

The dynamics that govern the time-dependent meridional overturning (thermohaline) circulation are not very well understood. Typically, one assumes that, in some averaged sense, the ocean will adjust similarly to the overturning of a non-rotating fluid under the action of gravity balanced by "friction" [e.g. Marshall et al. 2001a]. Then one expects the zonally averaged overturning to increase for an enhanced equator to pole density gradient. Figure 6c shows the NAO related

change in the surface buoyancy flux to be on the order of $10^{-8} \text{ m}^2 \text{ s}^{-3}$. A persistent positive NAO forcing for five years will enhance the surface density in the subpolar ocean by about 0.1 - 0.2 kg m^{-3} , which is about 3-5% of the equator to pole density gradient. Emerging 'theories' of the oceans' overturning circulation [e.g. Marotzke 1997] suggest that changes in the meridional overturning circulation depend on the equator to pole density gradient to the one-third power. Thus the NAO-induced changes in the air-sea buoyancy flux are expected to only have a 2% effect on the buoyancy driven overturning, i.e. about 0.5 Sv. However, changes in the upper ocean circulation can induce significantly larger buoyancy flux divergences. The high latitude convective regions, such as the Labrador Sea, have large horizontal mean and eddy induced fresh water flux divergences due to their proximity to the very fresh coastal water masses [e.g. Khatiwala and Visbeck 2000, Khatiwala et al. 2002]. Little is known about the interannual variability of those fresh water exchanges, but positive feedbacks have been identified. During a low NAO phase, the air-sea heat flux low and deep convection reduced. This removes the main sink for the surface freshwater from the shelf and thus surface freshwater builds up increasing the surface buoyancy further. This positive feedback has been proposed to be one of the possible mechanisms to generate or locally enhance a "Great Salinity Anomaly" [Rahmstorf et al 2001; Houghton and Visbeck 2002]. In summary, much less is known about the theoretically expected response of the buoyancy driven overturning circulation.

6.4.3 Response of the Oceans' Poleward Heat Transport due to circulation changes

The ocean plays several important roles in the climate system. First, the oceans large heat capacity results in local heat storage of air-sea flux imbalances and thus provides a temporal low pass filter on the response to changes in the forcing. Second, the ocean circulation assists the atmosphere in transferring excess heat from the tropics to the polar region (see also Czaja et al. [this volume] for a quantitative discussion). The ocean's poleward heat transport can be altered in two ways: changes in the thermal gradients ($\nabla T'$) within the ocean and/or changes in the circulation acting on the mean temperature gradient (∇T). Firstly we focus on the latter and show how changes in ocean circulation affect the oceans (poleward) heat transport.

In the Atlantic sector, much of the poleward heat transport is due to the meridional overturning circulation which advects warm water poleward in the surface layers balanced by a deep and much colder return flow. Simple scaling arguments can be used to estimate the main contributions to the circulation-induced changes in the poleward heat transport.

We will now discuss various ways how the NAO can change the ocean's poleward heat transport. There are two ways to proceed: First, we can try to estimate the contribution to the heat transport by changes in the ocean circulation (∇T). Secondly one can imagine that on long time scales the ocean might have to balance the net air-sea heat flux anomaly by a change in the circulation once it has "exhausted" its heat storage capacity.

The first and most rapid contribution is due to the Ekman transport induced vertical overturning, which can be estimated by:

$$Q_{\text{MOC,ek}} = \rho_0 c_p \Delta T_z \Phi_{\text{ek,max}},$$

where ρ_0 ($\sim 1025 \text{ kg m}^{-3}$) is a reference density, c_p ($\sim 4000 \text{ J kg}^{-1} \text{ }^\circ\text{C}^{-1}$) denotes the specific heat capacity of sea water and ΔT_z is the surface to deep temperature difference where the return flow is expected. We will assume that ΔT_z decreases monotonically from 18°C in the tropics to less than 5°C north of 60°N . Thus, we expect an increased poleward heat transport south of 40°N of a

maximum of 0.06 PW ($\Phi_{ek,max} \sim 1.5$ Sv, $\Delta T_z \sim 10^\circ\text{C}$ at 30°N), and a decrease between 45°N and 65°N with a minimum of -0.05 PW ($\Phi_{ek,max} \sim -2.5$ Sv, $\Delta T_z \sim 5^\circ\text{C}$ at 55°N).

The second contribution is due to changes in the horizontal gyre circulation and is estimated to be:

$$Q_{sv} = \rho_0 c_p \Delta T_x M_{sv},$$

where ΔT_x is the horizontal temperature difference which changes sign at the subpolar/subtropical gyre boundary and is expected to be on the order of 2°C . Thus we expect an increased poleward heat transport south of 50°N with a maximum of 0.05 PW ($M_{sv} \sim 6$ Sv, $\Delta T_x \sim 2^\circ\text{C}$ at 40°N), smaller values at the gyre boundaries, and increasing again north of 55°N with a maximum of 0.07 PW ($M_{sv} \sim 8$ Sv, $\Delta T_x \sim 2^\circ\text{C}$ at 60°N).

Finally, enhanced surface buoyancy loss in the subpolar regions plus contributions due to advection induces changes in the density field will accelerate the meridional overturning circulation (Φ_{max}). We have little way of knowing ahead of time its strength so as an educated guess we will assume that it might be as large as 15% or ~ 2 Sv:

$$Q_{MOC} = \rho_0 c_p \Delta T_z \Phi_{max},$$

Such an increase would enhance the poleward heat transport by about 0.05-0.08 PW everywhere south of 55°N .

In summary, we expect from consideration of ocean circulation theory that within weeks of a positive NAO index winter, the ocean heat transport will be altered by the Ekman driven component which will result in enhanced poleward heat transport south of 45°N of 0.05 PW. North of 50°N , the contribution due to the Ekman overturning will reduce the heat transport by about -0.05 PW. If the NAO forcing persists for a few consecutive winter seasons, the gyre response will grow and enhance the poleward heat transport in the subtropical region by 0.1 PW. In the subpolar region the gyre contribution will offset the Ekman overturning to a net positive anomaly of 0.03 PW. Finally, if the forcing persists even longer, the buoyancy driven meridional overturning is expected to contribute. Although we have no very good way to estimate its anomalous strength, we speculate that the maximum total heat transport anomaly in subtropical gyre might reach 0.15 PW, decreasing northward to 0.08 PW at 50°N and even smaller north of that.

We can compare those estimates to the zonally averaged and south to north integrated air-sea flux anomalies (Figure 7a). If the ocean was not able to store heat anomalies and the air-sea fluxes would not depend much on the ocean state, then we would expect both estimates to agree. All we can say at this point is that the expected pattern and magnitudes roughly agree with our estimate of ocean heat transport changes due to a positive NAO index of about 10% of its long term average.

One of the interesting results from the consideration of ocean heat transport anomalies is that the NAO induced ocean heat transport divergence in the subpolar gyre should warm the subpolar gyre. Thus the altered ocean circulation might be able to offset the local cooling (Figure 4a-c; and Figure 6a) and could possibly even change the sign of the SST response in the subpolar gyre.

6.4.4 The Ocean Circulation Response in Dynamical Ocean Models

General circulation ocean models have been used extensively to elucidate mechanisms of climate variability and the oceans' role in the North Atlantic Oscillation. Most experiments used either a coupled ocean-atmosphere-(sea ice-land) model where NAO like variability was internally generated, or ocean only models forced by a specified perturbation of the atmospheric state. Within the latter category, a large number of studies have been performed in which the ocean was initialized using a mean climatological state and forced with time-variable air-sea fluxes of momentum, heat, and freshwater [e.g., Halliwell 1998; Häkkinen 1999; Paiva and Chassignet, 2002].

The oceans' response to NAO-like forcing was then deduced by either looking at individual years with extreme NAO states [e.g. Seager et al. 2000], and/or performing joint SVD analyses to isolate the dominant mode of variability [e.g., Eden and Willebrand 2001; Paiva and Chassignet 2002]. Others have used a typical or idealized NAO forcing anomaly and investigated the model's response in a more systematic way [e.g., Visbeck et al. 1998; Krahnmann et al. 2001; Eden and Jung 2001; Eden and Willebrand 2001; Paiva and Chassignet 2002].

Simpler models have also been used to elucidate parts of the oceans' response. For example, Taylor and Gangopadhyay [2001] investigated the meridional displacement of the Gulf Stream using a one layer zonally averaged model. Given the NAO index and its projection on the winds, they were able to hindcast the meridional displacements of the Gulf Stream. Others [e.g. Cessi 2000; Weng and Neelin 1998] have used two-layer quasi-geostrophic models to study the delayed ocean response to NAO-like forcing focussing on the long Rossby wave adjustment process.

The more complete general circulation ocean models all show that the depth average response to the NAO wind forcing is qualitatively similar to the equilibrium Sverdrup response (Figure 7d), with a northeastward extension of the subtropical gyre. This anomaly pattern has been referred to as the 'inter-gyre gyre' by Marshall et al. [2001a]. The largest transport anomalies are found between 35° and 45°N with magnitudes of 3-4 Sv [e.g., Eden and Jung 2001] in good agreement with simple theory.

As predicted by theory, the response of the meridional overturning circulation to changes in the NAO index is more complicated. Häkkinen [1999] finds a reasonable correspondence of the meridional overturning circulation with the NAO index at 25°N. The modeled overturning circulation increases by about 3 Sv for a sustained positive NAO index phase. This is in good agreement with the expected rapid Ekman driven response, plus some contribution from the density driven circulation. However, the response north of 45°N is expected to be out of phase by the same arguments. Enhanced (reduced) transport at 55°N in the Deep Western Boundary Current (DWBC) was indeed observed in the modeling study of Paiva and Chassignet [2002] during periods of low (high) NAO index. Eden and Jung's calculation [2001, their Figure 5] also supports our prediction; however, they only comment on the multi-decadal frequency response, which lags the low frequency NAO index by 1-2 decades and is of the same sign. Häkkinen's [1999] model shows a very similar response, with an out of phase relationship between the meridional ocean heat transport south of 40°N versus north of 45°N for the high frequencies and an in phase response on decadal and longer time scales (her plate 1).

Visbeck et al. [1998] show a similar frequency-dependent response of the subpolar gyre, with cooling for interannual NAO wind forcing and warming for the low frequency response. However, they attribute part of that response to advection of the SST anomaly by the mean ocean currents [Krahnmann et al 2001].

Delworth and Dixon [2000] used a coupled ocean-atmosphere model to examine the impact of a sustained (multidecadal) positive phase of the NAO on the model's overturning circulation. Consistent with the above discussion they found an increase of the meridional overturning of approximately 2 Sv (14% of the mean) in response to a sustained positive phase of the NAO, corresponding to a 9 hPa increase in the gradient of SLP between the Azores and Iceland. This response was primarily due to NAO-related changes in the surface heat flux, leading to changes in the large-scale density field which acted to "spin up" the overturning circulation by increasing the meridional density gradient.

Although a complete theory for the meridional overturning circulation and poleward heat transport is not readily available, we have shown that progress can be made by a mechanistic approach to rationalize the modeled circulation and heat transport response to NAO like forcing. Such an approach has also been taken by Marshall et al [2001a] who provide a conceptual framework for thinking about the response of the ocean to NAO forcing that is phrased in delayed oscillator theory including possible feedback to the atmosphere. A similar approach is discussed in more detail by Czaja et al. [this volume]. In the following we will review what is known about ocean circulation changes from observations.

6.4.5 Observational Evidence for NAO Induced Circulation Changes

Hydrographic observations in the Atlantic Ocean can be used to study the low frequency response of the ocean (decadal and longer). In particular, the apparent trend of the NAO index that characterized the latter half of the twentieth century was echoed by a change of North Atlantic steric height and potential energy distributions [Levitus et al. 1990; Greatbatch et al. 1991; Curry and McCartney 2001]. The persistent 1960's low NAO index phase precipitated an 8-10 dyn cm drop in steric height of the subtropical gyre interior and a simultaneous rise in the subpolar gyre interior and slope water regions. The subsequent extended high NAO index phase culminated in the reverse situation in the 1990's: a 10 dyn cm rise of steric height in the western subtropical gyre opposing a 10 dyn cm drop in the western subpolar gyre. Since the meridional baroclinic pressure gradient drives eastward flow along the mutual boundary between the gyres -- i.e. the Gulf Stream and North Atlantic Current system -- these basin-scale shifts imply a gyre circulation that was alternately weakened and strengthened in these time periods. The altered potential energy distributions indicate baroclinic transport changes of $\pm 17\%$ [Greatbatch et al. 1991; Curry and McCartney 2001] amounting to approximately 8-10 Sv intensification of each gyre's transport when averaged over the upper 2000 meters between extremes (1970 and 1995).

Using long records of hydrographic observations from the Labrador Sea Basin and Bermuda, Curry and McCartney [2001] constructed a time history of baroclinic pressure difference between the subtropical and subpolar gyre centers (Figure 8c). With this index of eastward transport -- an oceanic analogue to the Iceland - Azores sea level pressure -- they demonstrated that the large scale ocean fluctuation was remarkably similar in its evolution between strong and weak phases and showed a similar temporal structure as the atmospheric NAO index. However, the two indices do not co-vary directly; as expected the ocean signal is delayed, and to first order, reflects a time integration of the atmospheric forcing. To some degree, the individual gyres' potential energy histories fluctuate in antiphase reflecting latitudinal shifts of surface westerlies associated with the NAO. But distinct forcing mechanisms and baroclinic responses in each gyre generate differences in the details of their respective histories (Figure 8a,b). The subpolar potential energy changes are primarily thermally driven through diabatic mixing and surface buoyancy fluxes associated with deep convection and the formation of Labrador Sea Water. By contrast, the interior subtropical gyre history is dominated by quasi-adiabatic (wind stress driven) vertical displacements of the main pycnocline. Sturges and Hong [1995] interpreted this signal as a first baroclinic mode response supplemented by the local air-sea heat flux variability and formation of

subtropical mode waters. Advective-diffusive import of Labrador Sea Water also contributes in significant amounts to the baroclinic transport fluctuation through its alteration of mid depth density structure and a growth and decay of deep geostrophic shear on interannual to decadal time scales.

This zero order description of the gyres circulation spinning up and down focuses on trends over fifty years in the western basins where integration of persistent atmospheric patterns produced sometimes large amplitude and deep-reaching ocean anomalies. Since sustained time series measurements of ocean currents are generally unavailable, e.g. for the Gulf Stream and North Atlantic Current, more quantitative assessments of circulation variability are limited in time and location. As mentioned above, the longest observational record of ocean flow is a 16-year time series of daily transport through Florida Strait derived from telephone cable voltages since 1983. In addition to a vigorous annual cycle, the Florida Current transport exhibits substantial long term variability [Baringer and Larsen 2001]: weakening by ~ 4 Sv between 1985 and 1992 and then progressively strengthening by ~ 4 Sv until 1998. The amplitude change and timing of the Florida Strait transport fluctuation are comparable to the subtropical thermocline transport change diagnosed from the Bermuda potential energy and sea level records for the same time period (Figure 8a). This relationship hints at the possibility that the flow through the Florida Strait may have been attenuated from recent values of 30-35 Sv to average values of only 25-30 Sv in the late 1960s when Bermuda sea level and dynamic height were also at a 50-year low.

Downstream from the Florida Current, the Gulf Stream exhibits north-south shifts in mean position that are coordinated with the NAO wind history [Taylor and Stephens 1998; Joyce et al. 2000; Frankignoul et al., 2001]. In high NAO index phases, the Gulf Stream separation point and mean flow path are distinctly northward, while the opposite southward situation is associated with a low index phase. These excursions are consistent with a Sverdrup response to latitudinal shifts of the zero wind stress curl line and adjustments to enhanced or diminished southward Ekman transports integrated across the basin [Parsons 1969; Veronis 1973; Gangopadhyay et al. 1992; Taylor and Stephens 1998]. As in the transport index fluctuation, the latter introduces an element of delay to the Gulf Stream response which is best correlated to the NAO wind forcing at lags of 0-2 years.

Compared to the subtropical gyre, NAO air-sea heat flux anomalies have much greater impact on the subpolar circulation through surface buoyancy forcing and water mass transformation that directly affects the upper 2000 meters or so of the Labrador Sea (see section 6.6.2). Thus, the persistent low NAO index and diminished subpolar air-sea heat fluxes of the 1960s was accompanied by decreasing vertical exchange in the interior Labrador Basin, warming LSW, increasing potential energy, and weakening of the gyre circulation. The opposite cooling, decreasing potential energy, and strengthening gyre attended periods of positive NAO and enhanced subpolar air-sea heat exchange. The persistence and amplitude of the high NAO index for several decades subsequent to 1972 culminated in extremes of these subpolar ocean properties in the mid-1990s.

Although the decadal varying strength of the subpolar gyre circulation is primarily a thermally driven phenomenon [Curry and McCartney 2001], variable fluxes of mass and fresh water from the Arctic contribute to these fluctuations, in perhaps more subtle, but nonetheless, significant ways. Enhanced Arctic outflows -- associated with periods of low NAO and anomalous northerly winds in the Canadian Archipelago and east of Greenland -- brought distinct pulses of fresh water and sea ice to the Labrador Sea in the mid-1960s, early 1980s, and late 1990s [Dickson et al. 1988; Belkin et al. 1998]. These outflows boosted the baroclinic transport of the 0-200 meter Labrador slope current, and infused the continental shelf with cold, fresh waters that lowered temperatures by 2-4°C all the way down to the Gulf of Maine [Petrie and Drinkwater 1993].

Their influence around the shallow periphery of the Labrador Sea in the 1960s and early 1980s coincided with periods of weakened gyre circulation and a relaxed dynamic height "bowl". This situation enabled lateral spreading of the cold, fresh Labrador slope waters across the surface of the basin interior that consequently interfered with convective activity and further weakened the gyre circulation. Consecutive winters of high NAO eventually caused the surface lid to become dense enough to overturn. Reinitiations of convection (1972 and 1985) dramatically altered LSW temperature, salinity, and potential energy characteristics and are reflected by rapid strengthening of the transport index (Figure 8c).

The cold, fresh upper ocean anomalies associated with Arctic outflows and possibly enhanced by local convective feedback [Houghton and Visbeck, 2002] eventually spread eastward from the Labrador slope through mixing with the North Atlantic Current [Reverdin et al. 1997; Belkin et al. 1998]. These episodes contrast starkly with opposite warm, saline upper ocean anomalies of subtropical origin that moved along the same pathway in the 1960s and 1990s. The surface expression of both warm and cold anomalies was captured by the SST analyses of Sutton and Allen [1997] and Hansen and Bezdek [1996]. Their arrival off the Ireland coast coincides with large excursions in upper ocean heat content and sea surface height observed in the eastern subpolar regions [Reverdin et al. 1997; Reverdin et al. 1999; Bersch et al. 1999; Esselborn and Eden 2001]. Unlike the delayed nature of the interior western basin signals relative to NAO wind forcing, the timing of these eastern changes coincides with -- and appears to be a more rapid response to -- latitudinal shifts of the zero wind stress curl line [Lorbacher 2000]. A possible mechanism for transmission of these anomalies into the eastern basins has been proffered in the context of Sverdrup dynamics altering the meridional transports of the underlying cold (subpolar) and warm (subtropical) circulation elements of the North Atlantic Current [Lorbacher 2000; Eden and Willebrand 2000; Esselborn and Eden 2001]. Acting upon the east-west baroclinic pressure gradient across the subpolar front, the cold anomaly of the early 1970s served to suppress intensification of the gyre for a few years subsequent to the 1972 NAO phase shift and, in the late 1990s, to delay its weakening following the 1996 drop in the NAO index.

Although the observational record is rather far from providing a complete picture of North Atlantic circulation history, there are enough glimpses to support a basic understanding of the ocean's large scale response to NAO forcing including significant fluctuations of gyre flows on the order of $\pm 15\%$. This results in a cycle of weakening and strengthening gyres and gives evidence for the strong integral power of the oceans circulation as well as the delayed nature of the response. Hence it becomes clear that the oceans' response involves more than one-dimensional mixed-layer processes. It suggests that anomalies of ocean heat advection and convergence play a roles in setting SST in particular near the strong transport and recirculation regimes of the Gulf Stream and North Atlantic Current as well as via the subpolar western boundaries that serve as conduits for outflows from the Arctic. Such anomalies could result from advection of heat and fresh water anomalies by the mean circulation or by an oceanic circulation that itself is anomalous.

6.5 ADVECTION OF ANOMALIES BY MEAN OCEAN CURRENTS

In the previous section, we discussed the wind and buoyancy driven changes of the ocean circulation due to the altered surface forcing. In most regions the velocity anomalies are on the order of 5-20% of the mean currents. In regions of large mean currents, however, we expect that the NAO induced temperature and salinity anomalies can be preferentially dispersed in the direction of the mean currents. This mechanism can provide a delayed non local response of sea surface anomalies.

6.5.1 SST propagation along the Gulf Stream / North Atlantic current

Studies of interannual SST variability have revealed the propagation of temperature anomalies within the North Atlantic Ocean [e.g., Hansen and Bezdek 1996]. While several pathways have been identified, the strongest signal was found along the pathway of the Gulf Stream/North Atlantic Current. Sutton and Allen [1997] hypothesized that this SST propagation might be predictable on decadal time scales. They showed statistically significant lag correlation of SST anomalies along the mean path of the GS/NAC with a 5-8 year lag between the subtropical and subpolar gyre. Note, however, that their "source" region between Florida and Cape Hatteras is not very strongly correlated with the NAO and that by using a longer data set the advection of anomalies seems to be less convincing [e.g. Krahnmann et al. 2001]. One of the puzzling aspects was the rather slow propagation speed of the anomalies on the order of 2 cm s^{-1} compared to the much swifter mean currents in the region. Theoretical work by Saravanan and McWilliams [1998] pointed to the strong control of air-sea coupling in this process and alluded to only limited predictive (deterministic) response. A comprehensive diagnostic of numerical experiments within an ocean general circulation model by Krahnmann et al. [2001] was able to verify the slow SST propagation speeds and showed that the apparent propagation speed is a strong function of the frequency of the forcing. For decadal modulation of the NAO index a propagation speed of $2\text{-}3 \text{ cm s}^{-1}$ was found consistent with the observed value. They hypothesize, however, that the slow propagation speed is due to strong air-sea heat flux damping of the anomalies.

A second key finding in their numerical simulations was that ocean dynamics, due to a combination of advection of temperature anomalies and increase of the GS/NAC, resulted in a switchover from an out of phase response between the subpolar and subtropical gyre (North Atlantic SST dipole) to a basin scale warming for persistence NAO forcing (> 15 years).

Can propagation of thermal anomalies be exploited for long term (5 year and longer) predictability of ocean SSTs? Frankignoul et al. [1998] diagnosed the strength of the air-sea flux damping in the North Atlantic and found it to be of order $20 \text{ W m}^{-2} \text{ K}^{-1}$, which suggests, that practical SST predictability will be limited to a few seasons due to the strong wintertime air-sea flux damping. However, the reemergence mechanism of Alexander and Deser [1995] would allow upper ocean heat content anomalies to prolong beyond the strong damping to possibly 2-3 years.

6.5.2 NAO induced water mass anomalies propagating along the deep western boundary current

The deep western boundary current (DWBC) system is synonymous with the cold limb of the North Atlantic meridional overturning circulation in returning cold, dense waters equatorward from the polar and subpolar basins to balance the poleward flow of upper ocean waters. It is the principal conduit by which climate signals, in the form of water mass perturbations, propagate from their high latitude source regions to the lower latitudes. Over the past four decades changes in the NAO index have resulted in significant changes in the character and production of deep waters in the Nordic and Labrador Seas -- the source waters of the DWBC. The observed changes of these water masses will be discussed in more detail in section 6.6, so here we focus on the timing and amplitude as the anomalies propagate into the subtropical and tropical deep ocean circulation.

The downstream effects of high latitude variability are recognizable as conspicuous shifts in temperature-salinity characteristics as well as changes in atmospheric tracer gas concentrations in the subtropical and tropical intermediate and deep circulation. Two distinct cores of recently ventilated (highest dissolved oxygen and CFC (Chlorofluorocarbons) concentrations) waters are

associated with maxima in the DWBC velocity distribution. The deepest, densest flows (Lower North Atlantic Deep Water) have origins in the Nordic Seas Overflow Waters, while the upper core (Upper North Atlantic Deep Water) is linked to waters formed by deep convection in the Labrador and possibly Irminger Seas. Although the DWBC is mainly constrained to flow adjacent to the continental slope, vigorous recirculations support advective-diffusive exchange of the recently ventilated waters with the basin interior.

Because multi-decadal time series measurements of DWBC flow are unavailable, little is known about its correlation (in phase or lagged) with the NAO index. The effects of NAO induced changes are most clearly discernible in the mid-depth western subtropical basin where Labrador Sea Water (LSW) directly influences the water properties. Cycles of warming and cooling below 1500 m are evident in zonal hydrographic sections at 24°N occupied in 1959, 1981, 1992, and 1998 [e.g. Parrilla et al., 1994]. Analysis of the Bermuda hydrographic time series indicates that these cycles are formally uncorrelated with changes in the overlying thermocline waters and include a 70-year warming trend of amplitude 0.5°C/century [Joyce and Robbins, 1996]. Curry et al. [1998] related both the trend and decadal fluctuations in the Bermuda 1500-2000 m temperature record to the Labrador Basin convective history. They suggested that the warming trend reflected a long term decline in LSW production and export of that water mass to the subtropics. Decadal persistence of a positive (negative) NAO index phase results in strong (weak) Labrador Basin convection, and enhanced (diminished) LSW export and was coordinated -- in a delayed fashion -- with smaller amplitude, basin-scale cooling (warming) episodes. The recent Bermuda record, updated to 2000 (Figure 9), supports these assertions, for it shows that the apparent warming trend has reversed to cooling -- 0.15°C since 1988 -- in response to the recent extreme phase of a positive NAO index and maximum LSW production.

The middepth subtropical response to Labrador Basin convection history is delayed by 5-10 years depending on distance along the spreading pathways [e.g. Curry et al. 1998; Molinari et al. 1998; Smethie et al. 2000]. Spreading rates appear also to be faster during LSW cooling episodes compared to warming events [Koltermann et al. 1999], an observation that is consistent with NAO-induced cycles of strong and weak gyre circulations [e.g. Curry and McCartney 2001].

A good overview of average spreading rates is provided by Smethie et al. [2000] who used CFC ratios to map spreading times and dilution rates for the LSW layer over the entire western basin. They show western-intensified spreading with transit times of ~15 years to arrive in the subtropical interior, 20 years to 20°N, and about 25 years to reach the equator, where the CFC signal bifurcates into east- and south-flowing components. Dilution increases with distance from the source ranging between factors of 2-4 for the subtropical circulation, and increasing to a factor of 10 in the tropics as the spreading path approaches the equator. These estimates translate to an effective spreading rate of 1-2 cm s⁻¹ for climate anomalies to penetrate the entire western North Atlantic.

Interdecadal cooling and freshening have also been observed in the deep Nordic Seas Overflow Waters (NSOW; see also section 6.6.3), but for a variety of reasons the subtropical and tropical manifestations of these perturbations have been much more subtle. Firstly, the overflows entrain considerable amounts of the ambient intermediate waters as they descend into the Iceland and Irminger Basins. Secondly, the coldest components of these NSOW (potential temperatures < 1.8°C) are recirculated to the north in the Newfoundland Basin, while only the warmer varieties are actually exported into the subtropical circulation. Thirdly, the Lower North Atlantic Deep Water (LNADW) is a mixture of tremendous volume comprising not only the exported NSOW but also Antarctic Bottom Waters. Thus any NAO induced temperature - salinity shifts are significantly subdued by the time they reach the subtropical DWBC. This is consistent with the observed cooling of approximately 0.05°C at LNADW levels between 1957 and 1992 at 24°N.

Ages derived from CFC ratios range from 12-15 years in the DWBC south of the Grand Banks and increase to 25-30 years near the 8°N. Thus we expect that anomalies the LNADW will be delayed by 10-15 years since their exit from the subpolar basin.

In order to investigate tracer anomaly propagation in the DWBC, Peng et al. [pers. comm. 2002] seeded CFCs in the Labrador Sea region in the North Atlantic model of Paiva and Chassignet [2002] during (a) a high NAO episode (1948-1950) and (b) a low NAO episode (1964-1966). In the low NAO index case, the tracers remain mostly north of 35°N after 20 years. This is to be contrasted with the high NAO episode where tracers are advected much more rapidly and reached 10°N after 20 years which is consistent with the detection of the CFC laden Labrador Sea Water recently detected at 26.5°N by Molinari et al. [1998] and the transit times diagnosed from the basin scale observations.

Whereas the above discussion focuses on advective propagation of NAO-related temperature (tracer) anomalies, Yang [1999] suggested planetary waves as a potential -- and more rapid -- mechanism that links the high and low latitudes. He documents a rather surprisingly strong 5-year lag correlation between the Labrador Basin convection history and phase of the cross equatorial SST gradient [see Marshall et al. 2001b for a review of tropical climate variability in the Atlantic sector] which greatly exceeded the cross-correlation of the NAO index and the tropical SST patterns. Using an idealized sector ocean model, he demonstrated that boundary waves, excited by oscillations in the meridional overturning strength, could directly alter cross-equatorial heat transports and generate a dipole pattern in tropical SST that was independent of local surface fluxes. However, this mechanism awaits confirmation in more realistic ocean model configurations.

We will now focus our attention on the dramatic changes of water masses in the North Atlantic Ocean that are most likely induced by the recent long term shift in the NAO index.

6.6 CHANGES IN WATER MASSES

The North Atlantic Ocean forms several important water masses. Their properties are characterized by the conditions at the sea surface. Changes in air-sea fluxes, interior ocean circulation, and ocean mixing can all alter the signature of a water mass in terms of temperature, salinity, and volume or layer thickness. In particular, the subtropical and subpolar mode waters have shown changes in their properties over the last several decades. Dickson [1997] and Dickson et al. [1996] contrasted the decade of the late 1960s when the NAO index was low to the decade of the 1990s. During a decade of low NAO index, deep winter mixing was enhanced in the subtropical mode water region and in the center of the Greenland Sea, while convection in the Labrador Sea was weak. This out of phase behavior is reproduced by several ocean models forced with the observed atmospheric state. For example in Paiva and Chassignet [2002], the simulated layer thickness anomalies in the western subtropics are, as in the observations, out-of-phase with those in the Labrador Sea. Layer thickness anomalies in the western subtropics and in the Labrador Sea were found to correlate well with the NAO at near-decadal time scales, with the oceanic response lagging the NAO by approximately 2-3 years. These results support the hypothesis, that changes in water mass formation in the western North Atlantic can be attributed, to a large extent, to changes in the pattern of the large scale atmospheric circulation, which generate sensible and latent heat flux variability by modifying the strength and position of the westerly winds. In the following, we review in more detail the observed changes of the ocean properties due to the multi-decadal trend in the NAO index.

6.6.1 Observed NAO induced changes in the Subtropical Mode Water

The most prominent type of Subtropical Mode Water (STMW) in the North Atlantic is the 18°C water found to the south of the Gulf Stream in the Sargasso Sea. Strong air-sea buoyancy loss gives rise to deep winter mixing and thus a thickening of the layer, which is balanced by a year round mixing due to mesoscale eddies. Joyce et al. [2000] describe the relation of changes in the thickness and stratification with atmospheric forcing. They derive an index based on the stratification at roughly 300m depth and find that it is highly correlated with the NAO index (correlation coefficient ~ 0.75) in the 3-15 year frequency band. During the high index phase of the NAO, the surface buoyancy flux is reduced and the continued action of the mesoscale eddies reduces the layer thickness of the 18°C water. Consequently, the stratification at 300m depth has increased at Bermuda with a lag of 0-1 years. Joyce et al. [2000] show that this upper ocean response cannot be explained by wind stress curl induced changes in the pycnocline depth.

Observations of long term subsurface variability in the North Atlantic are sparse (both in space and in time), and evidence of the associated forcing mechanisms is not yet conclusive. Levitus [1989] used historical hydrographic data to suggest that the observed changes in the intermediate layers (500 to 1300 meters) between the 1955-1959 and 1970-1974 pentads may be related to variations in the magnitude of the wind stress curl (and therefore in the intensity of the Ekman pumping and/or of the gyre transport). A few locations in the North Atlantic have been continuously monitored, providing long term records of water mass properties. Talley and Raymer [1982] and Joyce and Robbins [1996] have used data from the Panulirus station (32°10'N, 64°30'W) to show variability on interannual to near-decadal time scales in the formation rates and properties of STMW, or 18 degree water. STMW is formed by subduction through the base of the winter mixed layer, in a region of strong surface heat loss. However, Jenkins [1982] and Talley and Raymer [1982] were unable to strongly correlate this variability to surface heat flux anomalies [see Talley 1996 for a recent review]. Molinari et al. [1997] analyzed the temperature response in the upper 400m throughout the subtropical North Atlantic and found that much of the multiyear SST signal extends down to at least 300m in the western part of the subtropical gyre.

The modeling study of Paiva and Chassignet [2002] was able to reproduce quite well the observed layer thickness and isopycnal depth anomalies associated with STMW at Bermuda. In the latter study, heat storage and preconditioning of the convective activity were found to be the important factors for the generation of STMW variability, with persistent cold or warm conditions, associated with anomalous heat loss over the western subtropics, being more significant for the generation of the simulated variability than strong anomalous events in isolated years. The layer thickness anomalies were generated to the northeast of Bermuda, near the Gulf Stream front, and were advected within a large area in the western subtropics and the Sargasso Sea.

6.6.2 Observed NAO induced changes in the Labrador Sea Water.

As already shown, the period from the mid-1960s to the mid-1990s was a most unusual episode in the climatic history of the North Atlantic, one in which the winter NAO index evolved from extreme negative to extreme positive values that are apparently unprecedented in the instrumental record (e.g. Figure 2). The ocean's response to this long-sustained shift in atmospheric forcing has been of particular importance in the Labrador Sea.

The Labrador Sea is a critical location for the Earth's climate system. In its upper and intermediate layers, annual-to-decadal variations in the production, character and thickness of its convectively-formed Labrador Sea Water directly determine the rate of the Atlantic subpolar gyre

circulation [Curry and McCartney, 2001]. Through its deeper layers pass all of the deep and bottom waters that collectively form and drive the lower limb of the Atlantic meridional overturning circulation (MOC). Around its margins pass the two main freshwater flows from the Arctic Ocean to the North Atlantic (via the Canadian Arctic Archipelago and East Greenland Shelf) which have been implicated in model experiments with a slowdown or shutdown of the MOC [Rahmstorf and Ganopolski, 1999; Delworth and Dixon, 2000; IPCC, 2001].

During the past 3-4 decades, the entire water column of the Labrador Sea has undergone radical change (Figure 10). From 1966 to 1992, the overall cooling of the water column of the Labrador Sea was equivalent to a loss of 8 W m^{-2} continuously for 26 years, the overall freshening was equivalent to mixing-in an extra 6m of fresh water at the sea surface [Lazier 1981; 1988; 1995 and pers. comm.], and as a result, the steric height in the central Labrador Sea in the mid-1990s was typically *8-10 cm lower* than in the late 1960s. These are arguably the largest full-depth changes ever observed in the modern instrumental oceanographic record, exceeding in depth, breadth, duration and/or amplitude the variability reported from other sites of deep exchange--the Greenland Sea [Verduin and Quadfasel, 1999], the eastern Mediterranean [Lascaratos et al 1999], or that associated with the Weddell Polynya of the mid-1970s [Gordon, 1982].

The observed cooling is consistent with an upward trend in the NAO index, however, the small rate indicates that an increased poleward heat transport of the ocean is required to offset the expected air-sea heat loss of $20\text{-}30 \text{ W m}^{-2}$. In particular the addition of 6m of fresh water is not consistent with the P-E estimates presented in Figure 5b. Again changes in ocean circulation, enhanced mixing with shelf waters or increased fresh water export from the Arctic are required. Though the influence of the amplifying NAO on these changes is identifiable throughout the water column of the Labrador Sea, the specific mechanism of the ocean's response to the change in NAO forcing will have been different and certainly less direct in the deep and abyssal layers than in the upper water column, and so will be described separately below (Section 6.6.3).

In the upper and intermediate layers of the Labrador Sea to the limit of convection ($\sim 2300\text{m}$ depth), the long cooling and freshening tendency seems part of a coordinated pan-Atlantic pattern of convective activity [Dickson et al, 1996], in which the intensity of convection at the three main sites (Sargasso Sea, Labrador Sea and Greenland Sea) evolved with the NAO between opposite extrema. From the NAO minimum of the 1960's, when the ventilation of the Greenland Sea and Sargasso was at a maximum and that of the Labrador Sea was tightly capped, convective activity evolved towards the opposite extreme state in the early 1990s, in which convection in the Greenland Sea and Sargasso was suppressed but vertical exchange in the Labrador Sea was reaching deeper than previously observed.

The specific mechanism is thought to involve the sort of change in the distribution of Atlantic winter storm activity that has long been associated with opposite extreme states of the NAO [e.g. Rogers, 1990; Hurrell and Dickson, 2001], and which latterly brought an intense storminess and a record northwesterly wind stress to the Labrador Sea during winters of the early 1990s. The result was intensifying and deepening ventilation of the Labrador Sea, with a progressive cooling and freshening of LSW into the 1990s [Figure 10, from Igor Yashayaev, BIO, pers. comm.], and ultimately, during the deepest-reaching convection since 1992, to an increase in LSW density as convection began to excavate the cold but saline sublayer of North Atlantic Deep Water [Dickson et al 1996]. Thus by the early 1990s, LSW was fresher, colder, deeper and denser than at any other time in the history of deep measurements there.

These changes in the mode water of the Labrador Sea have a value in tracing-out the rates and pathways by which LSW-spreads across the basin [e.g. Sy et al. 1997]. However, their major importance is likely to lie in their influence on the Atlantic circulation itself. As Curry and

McCartney [2001] point out, the main North Atlantic Current is driven by the gradient of potential energy anomaly (PE') across the mutual boundary between the subtropical and subpolar gyres (see also section 6.4.5).

6.6.3 *Observed NAO influence in the Nordic Seas.*

Though their wider influence is certainly regulated by the gaps and passageways that form their connections to neighboring seas, the Nordic Seas are potentially important as a source of change for both the climatically-sensitive Arctic Ocean and for the northern overflows which feed the deep southgoing limb of the meridional overturning circulation (MOC).

Over the past four decades, as the NAO Index has undergone its record low-frequency shift, the hydrographic character of the Nordic Seas has been observed to change, in some cases beyond the range of our past experience. In one way or another, these extreme anomalies appear to have arisen through a changing balance, sense or pattern of "exchange". Four changes in particular are attributed in large part to the amplifying NAO index: (1) an increased Atlantic inflow accompanied by the poleward spread of warmth along the eastern boundary to the Barents Sea and Arctic Ocean. (2) Reduced convection in the Greenland Sea with effects on the water mass character and structure in the neighboring Norwegian Sea. (3) a widespread freshening of the upper 1-1.5 km of the Nordic Seas. (4) the transfer of this freshening signal to the deep and abyssal Atlantic via the two main overflows which cross the Greenland-Scotland Ridge.

Atlantic inflow to Nordic Seas.

Modern estimates based on direct measurements [e.g. Hansen and Osterhus 2000; Orvik et al. 2001] describe two main branches of inflow to the Norwegian Sea carrying a total mean transport of order 7 Sv (a third inflow of order 1 Sv passes north to the west of Iceland). The eastern branch appears as a narrow, topographically trapped current carrying order 4 Sv northward against the upper continental slope. The offshore branch takes the form of an unstable frontal jet about 400m deep and is less well measured in consequence, carrying an estimated transport of order 3 Sv into the central Norwegian Sea.

These two inflow streams thus tap-off only a small fraction of the Atlantic Water transport brought east by the North Atlantic Current, and the variations in inflow, at least for the main branch passing through the Faroe-Shetland Channel, are ascribed to changes in the local wind field rather than to the large-scale changes in the Atlantic gyre circulation, described above. As the dominant mode of sea-level pressure variability in the Atlantic sector, the NAO can be expected to be implicated in these changes, and in fact specific associations with NAO variability have been described for the inflow and subsequent northward transport of Atlantic Water through the eastern Norwegian Sea.

First, using a box inverse method, Dye [1999] use the century-long hydrography from the Faroe-Shetland and Nolso-Flugga standard sections to identify long-term changes in the upper layer transport through the Channel, continuously since 1946, discontinuously before that. Perhaps because the box inverse method does not, in this case, give complete access to the barotropic component, the transports calculated are no more than half of the order 4 Sv that we believe passes north along the Scottish Slope. However, this analysis does demonstrate a clear association between inflow and the NAO, with the upper-layer transport increasing steadily by a little more than 1 Sv after the mid-60s, in parallel with the NAO index; the Faroe - Shetland throughflow (or at least this component of it) was at a century-long maximum in the early 1990s. The hydrographic analysis of data from the Svinoy Section by Mork and Blindheim [2000] would appear to support this conclusion. They find that the NAO index is closely associated with the

temperature, salinity and transport variations on this Section, which intercepts the inflow some 350 km further north at 62°- 64° 40'N. They suggest that since 1978 (thus covering much of the recent long-period change in the NAO Index), the transport through the whole section has increased by 1.1 Sv, mostly in the eastern branch. The current may also have narrowed. Using the 35 isohaline as a proxy for its westward extent, Blindheim et al [2000] show that the width of the Norwegian Atlantic Current (NwAC) at 65° 45'N has been closely (inversely) correlated with the winter NAO Index since 1963 ($r=0.86$ for a 2 year delay). Since NAO-positive conditions are associated with a greatly strengthened southerly airflow west of Norway [see Dickson et al 2000, their Figure 2e], these changes in the transport and width of the NwAC are both in the expected sense.

At higher latitudes, by the late-80s-early 90s when the NAO index reached its interannual and interdecadal maximum, the superposition of a short-term warming event on the long-term warming trend meant that both inflow streams to the Arctic Ocean [through Fram Strait and the Barents Sea] were running between 1 and 2°C warmer than normal [Dickson et al 2000; Grotefendt et al. 1998]. Adlandsvik's barotropic transport model [Adlandsvik, 1989; Adlandsvik and Loeng, 1991; Loeng et al. 1997] suggests that the transport through the Barents Sea pathway may have increased by around a quarter at this time, and we have possible proxy evidence from sea-level records to suggest that the West Spitsbergen Current was similarly boosted [Dickson et al 2000].

Further north still, we see the effect of these changes in a warming and spreading of the Atlantic-derived sublayer across the Eurasian Basin of the Arctic Ocean [Quadfasel et al 1991; Carmack et al 1995; Aagaard et al, 1996; Swift et al, 1997; Carmack et al, 1997; Morison et al, 1998 a,b and in press; see also McLaughlan et al, 1996; Kolatschek et al, 1996]. There, Morison's comparison of SCICEX data with "climatology" showed that the Atlantic sublayer had shoaled and warmed by up to 2°C and extended in distribution by about 20% [Morison et al. 1998; Dickson 1999], so that the mutual front between waters of Pacific and Atlantic origin had shifted from the Lomonosov to the Alpha-Mendeleev Ridge.

Thus the warm, moist southerly airflow that is directed along the eastern boundary of the North Atlantic under these increasingly NAO-positive conditions is held responsible for driving a warmer [Dickson et al 2000], stronger [Dye 1999; Mork and Blindheim, 2000; Orvik et al 2001] and probably narrower [Blindheim et al, 2000] flow of Atlantic water northwards to the Barents Sea and into the Arctic Ocean [Quadfasel, 1991; Tereschenko, 1996; Grotefendt et al 1998; Morison, Aagaard and Steele, 1998].

Convection in the Greenland Sea

As with the Labrador Sea, a radical interdecadal change in the depth and intensity of open-ocean convection was a second major change to affect the Nordic Seas, part of the same coordinated pan-Atlantic pattern of convective activity driven by the changing NAO that we described earlier [Dickson et al, 1996; Verduin and Quadfasel 1999]. From the NAO-minimum of the 1960s, the intensity of deep convection in the Greenland Sea became progressively more suppressed as the NAO index amplified to extreme positive values in the early-to-mid 1990s. Schlosser et al [1991] estimate a (model-dependent) 80% \pm 10% reduction in deep water formation from the 0.47 Sv of the 1960's and '70's to the 0.1 Sv of the 1980's. At the same time, a steady deepening of intermediate and deep isopycnals in the Greenland Sea from the early 1980s [Boenisch et al 1997] provides evidence of a collapse of the "domed" density structure in the Greenland Sea as a reduced windstress curl [Jonsson 1991] supported a less intense cyclonic basin circulation there [Meincke, Jonsson and Swift 1992; Rudels and Quadfasel 1991]. Perhaps in compensation, there

is evidence of an increased influx of deep waters from the Arctic Ocean into the Greenland Sea basin at intermediate depths [Meincke and Rudels, 1995; Meincke, Rudels and Friedrich 1997].

In summary, the well-known cooling-warming cycle of deep water (>2000m) in the Greenland Sea since the late 1950s [Clarke et al, 1990], successively updated by Meincke, Jonsson and Swift, [1992]; Meincke and Rudels [1995]; Verduin and Quadfasel [1999], is conventionally interpreted as evidence of a changing balance between vertical and horizontal exchange processes; less conventionally, Visbeck and Rhein [2000] suggest from CFC evidence that enhanced diapycnal mixing over the rough topography of Mohn's Ridge rather than increased deep exchange through Fram Strait may provide a better explanation of recent changes in ventilation and character of the deep water.

Regardless of whether strong vertical exchange in the Greenland Sea gave way to enhanced lateral exchange with the Arctic Ocean or merely with its own boundaries, there seems to be clear evidence of an altered inter-basin exchange with deep waters of the Norwegian Sea (NSDW). Until the early 1990's, NSDW had exhibited a low-amplitude and lagged version of the temperature changes shown by GSDW itself [Osterhus and Gammelsrod, 1999], and coupled with locally-driven changes in the upper layers of the Norwegian Sea (see next section), the net result was a steady and protracted deepening of the mutual interface between the Norwegian Sea Arctic Intermediate Water (NSAIW) and Deep Water (NSDW) in the Norwegian Sea over the past 4 decades; such a change has significant implications for overflow transport (described below).

Freshening of the Nordic Seas

A third recent and notable change in these waters is a large-scale, large amplitude freshening that has taken place in the upper 1-1.5 km of the Nordic Seas. Once again, the cause is largely attributed to the amplifying NAO, but with a variety of area-specific mechanisms:

- a) The direct export of sea-ice from the Arctic Ocean is one such [Vinje et al. 1998; Kwok and Rothrock, 1999; Vinje 2001a, 2001b]. A combination of current measurements, upward-looking sonar and satellite imagery reveals that the annual efflux of ice through the western Fram Strait increased with the NAO to a record volume-flux of $4700 \text{ km}^3 \text{ yr}^{-1}$ in 1994-1995. Although the relationship is not robust in the longer-term, each 1-sigma increase in the NAO index since 1976 has been associated with an approximately 200 km^3 increase in the annual efflux of ice to the Greenland Sea [Dickson et al. 2000].
- b) Throughout the marginal ice-zone of the Nordic Seas, a steady decrease in the local late-winter production of sea-ice has accompanied the increasing trend in the NAO over the past 40 years [Deser et al. 2000; see also section 6.7].
- c) The extension of storm activity to the Nordic Seas under extreme NAO-positive conditions [Rogers 1990; Alexandersson et al. 1997] is calculated to increase precipitation along the Norwegian Atlantic Current by approximately 15 cm per winter compared with the equivalent NAO-negative conditions [Dickson et al. 2000; see also Figure 5].

Other factors and mechanisms have undoubtedly contributed to the long and gradual but dramatic freshening of the European subarctic seas in recent decades, most of them associated in some way with the amplifying NAO. Blindheim et al. [2000] describe a range of factors internal to the Nordic Seas, including an increased freshwater supply from the East Icelandic Current, the narrowing of the salty Norwegian Atlantic Current towards the Norwegian Coast, already described, and the effect of the steadily-deepening interface between the Arctic Intermediate Water and Deep Water in the Norwegian Sea. Though it is not yet possible to partition the recent freshening of the Nordic Seas into its individual contributory components, the change is

sufficiently widespread and has occurred over a sufficiently deep layer to affect the hydrographic character of both dense overflows crossing the Greenland-Scotland Ridge.

Changes in the overflows: the propagation of the high latitude climate signal to the deep Atlantic.

We can now complete the circuit begun in section 6.6.2 above by linking the changes observed in the upper layers of the Nordic Seas to those in the deep and abyssal layers of the Labrador Sea. In the lower water column of the Labrador Sea, in depths of 2300-3500 m, repeat hydrography has indicated a steady freshening over the past three to four decades (Figure 10). Since these deep and abyssal layers lie beyond the reach of deep convection, such a change cannot be due to local climate forcing. Instead, it is likely to reflect change in the system of overflows that ventilate these deepest layers or change in the waters they entrain, or most likely both.

Two main changes in the overflows have been described. First, hydrographic sections monitoring the outflow of Norwegian Sea Deep Water and Arctic Intermediate Water (NSDW and NSAIW) through the Faroe-Shetland Channel and Denmark Strait confirm that salinities have decreased almost linearly by 0.01 per decade since the mid 1970s [Turrell et al. 1999; Dickson et al. in press]. Both overflows, therefore, appear to be tapping-off the freshening signal of the upper Nordic Seas. Dickson et al. [2002] construct salinity time-series at intervals along the spreading pathways of both overflows where they descend from their sills into the deep and abyssal ocean, and conclude that the freshening rate of both was maintained against dilution on their long spreading paths to the Labrador Sea by entraining or mixing with waters that were themselves freshening at an equal or greater rate (e.g. LSW itself, already described). Second, in addition to a change in the hydrographic character of overflow, there may well have been a companion change in its transport, at least in the case of the eastern overflow. As Hansen, Turrell and Østerhus [2001] point out, the cold dense outflow through the Faroe-Shetland Channel is driven by the upstream slope of the isopycnals which intersect the bottom at the Faroe-Shetland sill. And since the critical $\sigma_t=28.0$ isopycnal has been steadily deepening with time at our benchmark OWS M site in the Norwegian Sea-- part of the deepening interface between NSAIW and NSDW already described-- they conclude that the coldest and densest part ($T < 0.3^\circ\text{C}$, $\sigma_t > 28.0$) of the overflow from the Faroe Bank Channel will have decreased by 20% since 1950. Such measurements as we have from the Denmark Strait give no sign of any compensating increase in the cold dense outflow through that sill [Girton et al. 2001].

The upshot is that in the deeper layers of the NW Atlantic, volumetric analysis of waters denser than $\sigma_{t,2}=36.84$ by Yashayaev [pers. comm. 2002] reveals a spectacular shift in the entire T-S relation between the late 60s and the late 90s (Figure 11, kindly provided by Igor Yashayaev, BIO Canada, pers. comm. 2002). Waters of this density will include the convectively-formed local variety of Subpolar Mode Water (LSW) as well as the deep (NEADW) and abyssal (DSOW) derivatives of both overflows. Though the NAO is not the sole driver of this change, we would now assert, nonetheless, that the long amplification of the NAO index since the 1960s is reflected in this change via a range of mechanisms, including its influence on convective intensity in both the Labrador Sea and Greenland Sea, its effect on oceanic exchanges between the North Atlantic and subarctic seas, and its broadscale control of the freshwater accession to the upper layers of the Nordic Seas from which the overflow waters are largely recruited.

We continue our discussion with a brief review of the sea ice response to changes in the NAO index.

6.7 THE SEA-ICE RESPONSE

As shown in the previous sections, the NAO has a profound influence on the atmospheric and oceanic circulation in the North Atlantic. One of the centers of action of the NAO is located near Iceland close to the winter maximum sea ice cover. This proximity and NAO related variability in the northward extension of the North Atlantic Current into the Greenland-Iceland-Norwegian (Nordic) Seas suggests that the Arctic sea ice cover and ice export is likely to be modified by changes in the phase of the NAO [Dickson et al. 2000]. Observations indeed show a strong correlation between winter sea ice extent and the NAO index (see Figure 12). The NAO can influence Arctic sea ice through several different processes [Deser et al. 2000]: (1) changes in the air-ice flux of momentum and heat and (2) changes in the divergence of the oceanic heat transport. Other mechanisms such as variations in cloud cover, which influence the Arctic radiation budget, might also play a significant role. Enhanced wind stress associated with a positive NAO index generally force the sea ice edge southward in the Labrador Sea and further to the northeast in the Barents Sea. The effects due to variations in air-ice-ocean heat fluxes are more complex. During a positive NAO index phase, strong winds bring more warm air masses towards the Nordic Seas and Arctic Ocean thus reducing the winter sea ice production. The associated changes in wind driven ocean circulation result in enhanced ocean advection of warm water into the Nordic Seas, in particular if the forcing persists over several subsequent winter seasons. Both mechanisms reduced sea ice cover similar to that caused by the direct response to changes in wind stress.

Unfortunately, reliable long data of Arctic sea ice are mostly restricted to the position of the sea ice edge during the pre satellite era and sea ice concentration thereafter. In addition, we have a few decades of satellite tracked sea ice motion, but only the Fram Strait (between Greenland and Spitzbergen) has a continuous record of ice thickness over several years [Vinje et al., 1997].

Recent studies of changes in Arctic sea ice coverage [e.g. Chapman and Walsh 1993, Cavalieri et al. 1997, Deser et al. 2000, Vinje 2001] have found a long term decrease of some 3% per decade, with the strongest signal occurring during the summer months. This warrants a short discussion of the role of the seasonal cycle. Modeling studies of Zhang et al. [2000] suggest that the NAO impacts the wintertime ice thickness in the Arctic which may then precondition the summer ice concentrations even in the absence of additional anomalous atmospheric forcing during the summer. This long-term decline of summer sea ice cover coincides with a period of an increase of the NAO index since the mid 1960s. The associated pattern is shown in Figure 12, calculated by regressing the sea ice concentration onto the NAO index. The pattern is very similar to the first empirical orthogonal function (EOF) of the sea ice variability shown by Deser et al. [2000] and shows a slight increase in sea ice extent in the Labrador Sea and a reduction in the Greenland and Barents Seas. The variation both in the sea ice extent EOFs and in the correlation with the NAO is mostly restricted to the North Atlantic sector. Though the correlation between the principal component (PC) of the first EOF of sea ice concentration and the NAO index is high ($r=0.63$), Deser et al. [2000] note that "individual winters can be radically different". The pattern in Figure 12 is thus mostly associated with the decadal variations in the NAO index.

Figure 13 shows the evolution of winter sea ice concentration for the three main subpolar regions: Labrador Sea, Greenland Sea, and Barents Sea as well as the NAO index. All time series show considerable variability on interannual to decadal time scales. Trends are weak in the Labrador and Barents Sea, while the Greenland Sea sea ice concentration is decreasing in response to the positive trend of the NAO index. Decadal variability of the NAO index is well mirrored in the respective sea ice concentration time series, with short or negligible lags (lagged correlation peak at 0 to 1 year lag).

The export of sea ice from the Arctic into the Nordic seas through the Fram Strait has revealed a pronounced variability of the ice volume transport [Vinje et al. 1997, Harder et al. 1998]. Note, that increased sea ice export has been proposed as the cause of the "Great Salinity Anomaly" in the 1970s [Dickson et al. 1988]. Harder et al. [1998] show that the ice transport is mainly a function of the southward wind component in Fram Strait. A positive NAO index generally causes increased northerly winds in this region, though occasionally a zonal shift in the low pressure center of the NAO leads to significant changes in the projection on the northerly wind direction. Such anomalous wind patterns are likely to be the cause of the "radically different winters" mentioned by Deser et al. [2000]. Dickson et al [2000] and Hilmer and Jung [2000], in particular, show how the east west shift of the Icelandic Low (which is part of the NAO index) alters Fram Strait ice export by both changes in the local atmospheric pressure gradient as well as thermodynamically induced variations in sea ice concentration.

Thus we have two competing mechanisms that can both effect the sea ice concentration in the Greenland Sea: The large scale EOF pattern indicates that a positive NAO results in decreased ice cover. While NAO induced changes in Fram Strait ice export, which is the main source for the Greenland Sea sea ice, suggest increased ice export during the positive NAO index phase. This apparent paradox might be related to the different time scales on which the two different processes are important. The ice transport shows high correlation with the NAO index on short time scales, the larger scale ice concentration response pattern (first EOF) shows better correlation with the decadal and longer NAO variations. This difference is also apparent in the very high winter-to-winter autocorrelation of the first PC of 0.69 [Deser et al., 2000] and the lower correlation of the NAO index for the same time period of only 0.43. In addition to the east-west shift of the low pressure center one might speculate that an alternative possible explanation can be given by the slow response of ocean dynamics to the NAO forcing which would result in increased advection of warm waters from the North Atlantic into the Nordic seas. More research is needed to substantiate both arguments.

6.8 SUMMARY AND DISCUSSION

The ocean's response to changes in the phase of the NAO has been of interest since the discovery of the phenomena. Early investigators were convinced that the changes in the oceans' sea surface temperature and associated air-sea heat fluxes would have a significant impact on the atmospheric state and thus might reinforce or control the phase of the NAO. In recent years extensive numerical experimentation with a large range of atmosphere and climate models has been performed to quantify how strong this feedback might be. And although there is still disagreement between the various models and experiments the consensus seems to be a modest feedback from the ocean back to the atmosphere [Kushnir et al. 2002; Czaja et al. this volume].

We have argued, however, that the ocean's role seems to be more important on longer time scales. To date, because of the expense to runs such experiments, only very few studies have addressed coupling on decadal and longer time scales [e.g. Delworth 1996, Delworth and Dixon 2000]. While the coupled problem is interesting, we have restricted this discussion to the oceans response to atmospheric NAO-like forcing by combining insights gained from observations, theory, and results from general circulation ocean models.

Ocean and climate observations became more abundant between the late sixties until the turn of the century. That period was characterized by a trend in the NAO index punctuated with several strong interannual events. This has resulted in spectacular records of climate variability and change. However, as discussed in this chapter, the NAO can only partially explain the

observations' variability. This is mostly due to the fact that both theory and models indicate a rapid and slow response of the ocean to a change in the NAO index and that other modes of forcing can induce variability in the climate system.

On interannual time scales, NAO-induced changes in air-sea heat fluxes dominate the SST response and thus produce a well known response pattern (Figure 1; SST tripole). This has led several investigators to conclude that, to a first order, the ocean's response can be understood in terms of a one dimensional mixed layer response in good agreement with Hasselmann's [1976] stochastic climate model theory. However, we have shown here that, not only are the Ekman transport anomaly induced heat and fresh water flux divergences significant, but also the important role of the ocean's mean and variable geostrophic circulation in modifying the oceans sea surface temperature response. The lack of high quality basin scale air-sea flux measurements of heat and fresh water make it difficult to give precise ratios between local air-sea flux atmospheric forcing and changes due to slowly adjusting ocean currents, which are often remotely forced.

We have also shown that the ocean response to NAO forcing is strongly dependant upon the frequency of the forcing. Figure 14 shows in a somewhat schematic way how one can summarize the high frequency (interannual, left) and low frequency (decadal and longer, right) response of the upper ocean. If the NAO index persists for several winter seasons, a more complex response due to changes in ocean circulation emerges. The strength and position of the boundary currents respond with a delay between 0-3 years, while the ocean meridional overturning seems to take up to a decade to adjust. Preferential dispersion of temperature (property) anomalies along the pathway of mean currents also takes several years to show significant effects. All of these slow changes, mostly non-local, are the result of adjusting ocean dynamics and modify the ocean's response to the NAO. From theory, one would anticipate that it will take several decades to obtain a converged equilibrium response of the ocean. This time scale is set by the time it takes to ventilate the upper ocean water masses and for long planetary waves to communicate changes in pressure gradients across the ocean basin.

While the Atlantic is one of the best observed ocean basins, we still lack enough direct measurements of ocean circulation changes at depth and especially of the evolution of the three-dimensional salinity field. Fresh water exchanges with the Arctic Ocean are believed to be a key process and are not faithfully represented in the current generation of ocean and climate models. At this point in time, we can only speculate on what might have caused the observed decrease of salinity in the Labrador Sea which is equivalent to an input of 6 meters of fresh water. Our best estimate of local precipitation versus evaporation can not even explain a sizeable fraction of this signal.

There is mounting evidence that slowly adjusting ocean dynamics and advection of temperature anomalies can yield to a change of sign of the subpolar gyre temperature response to NAO forcing. Ocean model experiments [Visbeck et al. 1998, Krahnmann et al 2001, Eden and Willebrand 2000, Eden and Jung 2001, Delworth and Dixon 2000] have shown basin wide warming of upper ocean temperatures for sustained (low frequency) NAO forcing (see also Figure 14). The switch over from a cold subpolar gyre during a positive NAO index phase to a warmer than normal state seems to occur if the positive phase persists for more than 6-8 years. The emerging consensus is that both advection of thermal anomalies along the GS/NAC and an increase in the Atlantic meridional overturning circulation are responsible for the subpolar gyre warming in equal parts [Eden, pers. comm.]. Such insights are important when ocean properties are used to reconstruct climate changes of the past.

Table 1 lists changes in observed ocean properties that have been identified with the North Atlantic Oscillation. Table 1 of Marshall et al [2001b] provides a brief summary of how those changes in the physical climate system yield to societal impacts of the NAO [see also Drinkwater et al., this volume; Mysterud et al., this volume; and Straile et al., this volume]. In particular, Drinkwater et al. [this volume] review the impact of the NAO on the marine ecosystem where changes in the physical properties of the ocean are felt most directly. The marine ecosystem plays also a role in the cycling of carbon in the North Atlantic Ocean. Changes in the NAO index, for example, have been shown to directly effect primary productivity and the biological export of carbon [e.g. Dutkiewicz et al. 2001, Oschlies 2001]. Changes in the ocean mixed layer depths and surface buoyancy fluxes will directly effect the subduction rate [Marshall et al. 1993; Joyce et al. 2000, Marsh 2000] and thus the ventilation pattern and strength of the thermocline. All of those directly affect the ocean uptake of CO₂ and other gases.

The combination of theory, numerical models, and observations has allowed us to review the basic response of the ocean circulation to NAO-induced forcing. However, several of the mechanisms await final observational and/or theoretical proofs. Competing hypothesis are being offered to explain the same phenomena. We expect to gain new insights from the next generation of data assimilating climate models that will allow a more complete, three dimensional, description of the variability of the present and past. The oceans response to the NAO is also a key ingredient in the development of conceptual and numerical predictive models of the coupled climate system [see also Czaja et al, this volume; and Rodwell, this volume] to tackle problems such as global climate change [Gillett et al, this volume, IPCC 2001].

Acknowledgement

We acknowledge conversations with countless colleagues at numerous meetings over the past years as well as insightful comments from the four reviewers. This work would have not been possible without the generous support of our funding agencies in the US and Europe.

References

- Aagaard K., L. A. Barrie, E. C. Carmack, C. Garrity, E. P. Jones, D. Lubin, R. W. Macdonald, J. H. Swift, W. B. Tucker, P. A. Wheeler and R. H. Whritner 1996. US, Canadian researchers explore Arctic Ocean. *EOS*, **77** (22), 209 and 213.
- Adlandsvik, B., 1989. Wind-driven variations in the Atlantic Inflow to the Barents Sea. ICES CM 1989/C:**18** 13 pp (mimeo).
- Adlandsvik, B., and H. Loeng, 1991. A study of the climate system in the Barents Sea. *Polar Res.*, **10**, 45-49.
- Alexander, M. A., and C. Deser, 1995: A mechanism for the recurrence of winter time midlatitude SST anomalies. *J. of Phys. Oceanogr.*, **25**, 122-137.
- Alexandersson, H., T. Schmith, K. Iden, and H. Tuomenvirta, 1998. Long-term variations of the storm climate over NW Europe. *The Global Ocean Atmosphere System*, 6, 97-120
- Baringer, M.O. and J.C. Larsen, 2001: Sixteen years of Florida Current transport at 27N. *Geophys. Res. Lett.*, **28**: 3179-3182.

- Battisti, D. S., U. S. Bhatt, and M. A. Alexander, 1995: A modeling study of the interannual variability in the wintertime North Atlantic Ocean. *J. Climate*, **8**, 3067-3083.
- Belkin, I.M., S. Levitus, J.I. Antonov, and S.-A. Malmberg, 1998: "Great Salinity Anomalies" in the North Atlantic. *Prog. Oceanogr.*, 41, 1-68.
- Bersch, M., J. Meincke, and A. Sy, 1999: Interannual thermocline changes in the northern North Atlantic 1991-1996. *Deep-Sea Res. II*, 46, 55-75.
- Bjerknes, J., 1964: Atlantic air-sea interactions. *Advances in Geophysics*, **10**, 1-82.
- Blindheim, J., V. Borovkov, B. Hansen, S. -A. Malmberg, W. R. Turrell and S. Osterhus, 2000. Upper layer cooling and freshening in the Norwegian Sea in relation to atmospheric forcing. *Deep-Sea Res. I*, 47, 655-680.
- Boenisch, G., J. Blindheim, J. L Bullister, P. Schlosser and D. W. R. Wallace. 1997. Long-term trends of temperature, salinity, density and transient tracers in the central Greenland Sea. *J. Geophys Res.*, 102, 18553-18571.
- Carmack, E. C., R. W. Macdonald, R. G. Perkin, F. A. McLaughlin and R. Pearson, 1995. Evidence for warming of Atlantic water in the southern Canadian Basin of the Arctic Ocean: Results from the Larsen-93 Expedition, *Geophys. Res. Ltrrs.*, **22**(9), 1061-1064.
- Carmack, E. C., K. Aagaard, J. H. Swift, R. W. Macdonald, F. A. McLaughlin, E. P. Jones, R. G. Perkin, J. N. Smith, K. M. Ellis and L. R. Kilius, 1997. Changes in Temperature and Tracer Distributions within the Arctic Ocean: Results from the 1994 Arctic Ocean Section. *Deep-Sea Res. II*, **44** (8) 1487-1502.
- Cavaleri, D. J., P. Gloersen, C. L. Parkinson, J. C. Comiso, and H. J. Zwally, 1997: Observed hemispheric asymmetry in global sea ice changes. *Science*, **278**, 1104-1106.
- Cayan, D. R., 1992a: Latent and sensible heat flux anomalies over the northern oceans: Driving the sea surface temperature. *J. Phys. Oceanogr.*, **22**, 859-881.
- Cayan, D. R., 1992b: Latent and sensible heat flux anomalies over the northern oceans: The connection to monthly atmospheric circulation. *J. Climate*, **5**, 354-369.
- Chapman, W.L. and J.E. Walsh 1993: Recent variations of sea ice and air temperature in high latitudes. *Bull. Amer. Meteor. Soc.*, **74**(1), 33-47.
- Clarke, R. A., J. H. Swift, J. A. Reid and K. P. Koltermann 1990. The formation of Greenland Sea Deep Water: Double diffusion or deep convection? *Deep-Sea Res.*, **37**, (9), 1385-1424.
- Cessi, P. 2000: Thermal feedback on wind stress as a contributing cause of climate variability. *J. Climate*, **13**, 232-244.
- Curry, R. G., M. S. McCartney, and T. M. Joyce, 1998: Oceanic transport of subpolar climate signals to mid-depth subtropical waters. *Nature*, **391**, 575-577.
- Curry, R.G. and M.S. McCartney, 2001: Ocean Gyre Circulation Changes Associated with the North Atlantic Oscillation. *J. Phys. Oceanogr.*, **31**: 3374-3400.

- Czaja A. and J. Marshall, 2001: Observations of Atmosphere - Ocean coupling in the North Atlantic. *Quart. J. of the Roy. Meteor. Soc.*, **127**, 1893-1916.
- Czaja A., A.W. Robertson, T. Huck: The role of Atlantic ocean-atmosphere coupling in affecting North Atlantic Oscillation variability, this volume.
- Delworth, T. L., 1996: North Atlantic interannual variability in a coupled ocean-atmosphere model. *J. Climate*, **9**, 2356-2375.
- Delworth, T. L. and R. J. Greatbatch, 2000: Multidecadal thermohaline circulation variability driven by atmospheric surface flux forcing. *J. Climate*, **13**, 1481-1495.
- Delworth, T.L., and K.W. Dixon, 2000: Implications of the recent trend in the Arctic/North Atlantic Oscillation for the North Atlantic thermohaline circulation. *J. Climate*, **13**, 3721-3727.
- Deser, C., and M. L. Blackmon, 1993: Surface climate variations over the North Atlantic Ocean during winter: 1900-1993. *J. Climate*, **6**, 1743-1753.
- Deser, C., J. E. Walsh, M. S. Timlin, 2000: Arctic Sea Ice Variability in the Context of Recent Atmospheric Circulation Trends. *J. Climate.*, **13**, 617-633.
- Dickson, R.R., J. Meincke, S.A. Malmberg and A.J. Lee (1988) The "Great Salinity Anomaly" in the northern North Atlantic 1968-1982. *Prog. Oceanogr.*, **20**, 103-151.
- Dickson, R. R., 1997: From the Labrador Sea to global change. *Nature*, **386**, 649-650.
- Dickson, R. R., 1999: All change in the Arctic. *Nature*, **397**, 389-391.
- Dickson, R. R., J. Meincke, I. Vassie, J. Jungclaus, and S. Osterhus, 1999: *Nature*, **397**, 243-246.
- Dickson, R. R., J. Lazier, J. Meincke, P. Rhines, and J. Swift, 1996: Long-term co-ordinated changes in the convective activity of the North Atlantic. *Prog. Oceanogr.*, **38**, 241-295.
- Dickson, R. R., T. J. Osborn, J. W. Hurrell, J. Meincke, J. Blindheim, B. Adlandsvik, T. Vigne, G. Alekseev, and W. Maslowski. 2000. The Arctic Ocean Response to the North Atlantic Oscillation. *J. Climate*, **13**, 2671-2696.
- Dickson, R. R., I. Yashayaev, J. Meincke, W. Turrell, S. Dye, and J. Holfort. 2002. Rapid Freshening of the Deep North Atlantic over the past Four Decades. *Nature*, 2002
- Dutkiewicz, S., Follows, M.J., J.C. Marshall and W.W. Gregg, 2001: Interannual variability of phytoplankton abundance in the North Atlantic. *Deep-Sea Res. II.*, **48**, 2323-2344.
- Drinkwater, K.F., A. Belgrano, Á. Borja, A. Conversi, M. Edwards, C.H. Greene, G. Ottersen, A. J. Pershing, and H.A. Walker, The Response of Marine Ecosystems to Climate Variability Associated with the North Atlantic Oscillation, this volume.
- Dye S., A Century of variability of flow through the Faroe-Shetland Channel. 1999. PhD thesis University of East Anglia, 189pp.

- Eden, C. and T. Jung, 2001: North Atlantic interdecadal variability: Oceanic response to the North Atlantic Oscillation (1865-1997). *J. Climate*, **14**, 676-691.
- Eden, C. and J. Willebrand, 2001: Mechanism of interannual to decadal variability of the North Atlantic circulation. *J. Climate*, **14**, 2266-2280.
- Esselborn, S. and C. Eden, 2001: Sea Surface Height changes in the North Atlantic Ocean related to the North Atlantic Oscillation. *Geophys. Res. Lett.*, **28**, 3473-3476.
- Frankignoul, C., A. Czaja, and B. L'Hevender, 1998: Air-sea feedback in the North Atlantic and surface boundary conditions for ocean models. *J. Climate*, **11**, 2310-2324.
- Frankignoul, C. and K. Hasselmann, 1977: Stochastic climate models. Part 2. Application to sea-surface temperature variability and thermocline variability, *Tellus*, **29**, 284-305.
- Frankignoul, C., G. de Cotlogon, T.M. Joyce, S. Dong, 2001: Gulf Stream variability and ocean-atmosphere Interactions. *J. Phys. Oceanogr.*, **31**, 3516-3529.
- Gangopadhyay, A., P. Cornillon, and R.D. Watts, 1992: A test of the Parsons - Veronis hypothesis on the separation of the Gulf Stream. *J. Phys. Oceanogr.*, **22**, 1286 - 1301.
- Gillett, N. P., H. F. Graf, and T. J. Osborn: Climate Change and the North Atlantic Oscillation, this volume.
- Girton, J. B., T. B. Sanford and R. H. Kase, 2001. Synoptic sections of the Denmark Strait Overflow. *Geophys. Res. Lett.*, **28**, (8) 1619-1622.
- Gordon A 1982. Weddell Deep Water variability. *J. Mar. Res*, **40**, 199-217
- Greatbatch, R.J., A.F. Fanning, A.G. Goulding, and S. Levitus, 1991: A diagnosis of interpentadal circulation changes in the North Atlantic. *J. Geophys. Res.*, **96**, 22009-22023.
- Grotefendt K., K. Logemann, D. Quadfasel, and S. Ronski, 1998. Is the Arctic Ocean warming? *J. Geophys. Res.* **103**, 27,679-27,687
- Grötzner, A., M. Latif, and T. P. Barnett, 1998: A decadal climate cycle in the North Atlantic Ocean as simulated by the ECHO coupled GCM. *J. Climate*, **11**, 831-847.
- Hansen, D. V., and H.F. Bezdek, 1996: On the nature of decadal anomalies in North Atlantic Sea Surface Temperature. *J. Geophys. Res.*, **101**, 9749-9758.
- Hansen, B., and S. Osterhus, 2000. North Atlantic-Nordic Seas exchanges. *Prog. Oceanogr*, **45**, 109-208.
- Hansen, B., W. R. Turrell and S. Osterhus, 2001. Decreasing overflow from the Nordic seas into the Atlantic Ocean through the Faroe-Shetland Channel since 1950. *Nature*, **411**, 927-930.
- Häkkinen, S., 1999: Variability of the simulated meridional heat transport in the North Atlantic for the periods 1951-1993. *J. Geophys. Res.*, **104**, 10,991-11,007.
- Halliwell, G., 1998: Simulation of North Atlantic decadal/multidecadal winter SST anomalies driven by basin-scale atmospheric circulation anomalies. *J. Phys. Oceanogr.*, **28**, 5-21.

Hansen, D. V., and H. F. Bezdek, 1996: On the nature of decadal anomalies in North Atlantic sea surface temperature. *J. Geophys. Res.*, **101**, 8749-8758.

Harder, M., P. Lemke, and M. Hilmer, 1998: Simulation of sea ice transport through Fram Strait: natural variability and sensitivity to forcing. *J. Geophys. Res.*, **103** (C3), 5595-5606.

Hasselmann, L., 1976: Stochastic climate models: Part I: theory. *Tellus*, **28**: 289-305.

Hilmer, M. and T. Jung, 2000: Evidence for a recent change in the link between the North Atlantic Oscillation and Arctic sea ice export. *Geophys. Res. Lett.*, **27**(7), 989-992.

Houghton, R. W., 1996: Subsurface quasi-decadal fluctuations in the North Atlantic. *J. Climate*, **9**, 1363-1373.

Houghton, B. and M. Visbeck, 2002: Quasi-decadal salinity fluctuations in the Labrador Sea. *J. Phys. Oceanogr.*, **32**, 687-701.

Hurrell, J. W., 1995: Decadal trends in the North Atlantic Oscillation: Regional temperatures and precipitation. *Science*, **269**, 676-679.

Hurrell, J. W., and H. van Loon, 1997: Decadal variations in climate associated with the North Atlantic Oscillation, *Climate Change*, **36**, 301-326.

Hurrell, J.W., Y. Kushnir, and M. Visbeck, 2001: The North Atlantic Oscillation. *Science*, **291**, No. 5504, 603-605.

Hurrell J. W. and R R. Dickson 2001. Climate Variability over the North Atlantic. In: N. C. Stenseth, G. Ottersen, J. W. Hurrell, and A. Belgrano (Eds.) Ecological effects of climate variations in the North Atlantic. Oxford University Press in press.

Hurrell, J.W., Y. Kushnir, G. Ottersen and M. Visbeck, An Overview of the North Atlantic Oscillation, this volume.

IPCC, 2001. Climate Change 2001: The Scientific Basis. J. T. Houghton, Y. Ding, D.J. Griggs, M. Noguer, P. J. van der Linden and D. Xiaosu (Eds.), Contribution of Working Group I to the Third Assessment Report of the Intergovernmental Panel on Climate Change (IPCC) Cambridge University Press, UK. pp 944.

Jenkins, W. J., 1982: On the climate of a subtropical ocean gyre: decade time scale variations in water mass renewal in the Sargasso Sea. *J. Mar. Res.*, 42(S), 265-290.

Jones, P. D., T. J. Osborn, and K. R. Briffa: Pressure-based measures of the North Atlantic Oscillation (NAO): A comparison and an assessment of changes in the strength of the NAO and in its influence on surface climate parameters, this volume.

Jónsson, S. 1991. Seasonal and interannual variability of wind stress curl over the Nordic Seas. *J. Geophys. Res.*, **96**: C2, 2649-2659.

Joyce, T. M. and P. Robbins, 1996: The long-term hydrographic record at Bermuda. *J. Climate*, **9**, 3121-3131.

- Joyce, T. M., C. Deser, and M. A. Spall, 2000: The relationship between decadal variability of Subtropical Mode Water and the North Atlantic Oscillation. *J. Climate*, **13**, 2550-2569.
- Kaplan, A., M. Cane, Y. Kushnir, A. Clement, B. Blumenthal, B. Rajagopalan, 1998: Analyses of global sea surface temperature 1856-1991. *J. Geophys. Res.*, **103**, 18567-18589.
- Kaplan, A., Y. Kushnir, M. Cane, and M.B. Blumenthal, 1997: Reduced space optimal analysis for historical data sets: 136 years of Atlantic sea surface temperatures. *J. Geophys. Res.*, **102**, 27835-27860.
- Khatiwala, S. and M. Visbeck, 2000: An estimate of the eddy-induced circulation in the Labrador Sea., *Geophys. Res. Lett.*, **27**, 2277-2280.
- Khatiwala, S., P. Schlosser, and M. Visbeck, 2002: Tracer Observations in the Labrador Sea. *J. Phys. Oceanogr.*, **32**, 666-686.
- Kolatschek, J., H. Eicken, V. Yu. Alexandrov and M. Kreyscher, 1996. The sea-ice cover of the Arctic Ocean and the Eurasian marginal seas: A brief overview of present day patterns and variability. Pp. 2-18 in: R. Stein, G. I. Ivanov, M. A. Levitan and K. Fahl (Eds), *Berichte zur Polarforschung*, **212**, Alfred-Wegener Institute für Polar und Meeresforschung, Bremerhaven, Germany.
- Koltermann, K.P., A.V. Sokov, V.P. Tereschenkov, S.A. Dobroliubov, K. Lorbacher, A. Sy, 1999. Decadal changes in the thermohaline circulation of the North Atlantic. *Deep-Sea Res.*, **46**, 109-138.
- Kushnir, Y., 1994: Interdecadal variations in North Atlantic sea surface temperature and associated atmospheric conditions. *Journal of Climate*, **7**, 142-157.
- Kushnir, Y., W. A. Robinson, I. Blade, N. M. J. Hall, S. Peng and R. Sutton, 2002: Atmospheric GCM response to extratropical SST anomalies: Synthesis and evaluation., *Journal of Climate*, in press.
- Krahmann, G., M. Visbeck and G. Reverdin, Formation and propagation of temperature anomalies along the North Atlantic Current., *J. Phys. Oceanogr.*, **31**, 1287-1303, 2001.
- Kwok, R., and D.A. Rothrock, 1999. Variability of Fram Strait Ice Flux and the North Atlantic Oscillation. *JGR-Oceans*, **104**, 5177-5189.
- Lascaratos, A., W. Roether, K. Nittis and B. Klein. Recent changes in deep water formation and spreading in the eastern Mediterranean Sea. 1999. *Prog. Oceanogr.*, **44**, 5-36.
- Lazier, J. R. N., 1981: Oceanographic conditions at O.W.S. Bravo. *Atmos.-Ocean*, **18**, 227-238.
- Lazier, J. R. N., 1988: Temperature and salinity changes in the deep Labrador Sea, 1962-1986. *Deep Sea Res.*, **35**, 1247-1253.
- Lazier, J. R. N. 1995. The Salinity Decrease in the Labrador Sea over the Past Thirty Years. In: Natural Climate Variability on Decade-to-Century Time Scales. D. G. Martinson, K. Bryan, M. Ghil, M. M. Hall, T. M. Karl, E.S Sarachik, S. Sorooshian, and L. D. Talley, (eds.). National Academy Press, Washington, D.C. pp 295-304.

- Levitus, S., 1989: Interpentadal variability of temperature and salinity at intermediate depths of the North Atlantic ocean, 1970-1974 versus 1955-1959. *J. Geophys. Res.*, **94**, 6091-6131.
- Levitus, S., 1990. Interpentadal variability of Steric Sea level and geopotential thickness of the North Atlantic Ocean, 1970-1974 versus 1955-1959. *J. Geophys. Res.*, 95: 5233-5238.
- Loeng, H., V. Ozhigin and B. Adlandsvik, 1997. Water fluxes through the Barents Sea. *ICES J. Mar. Sci.*, **54**, 310-317.
- Lorbacher, K., 2000. Niederfrequente Variabilitaet meridionaler Transporte in der Divergenzzone des nordatlantischen Subtropen- und Subpolarwirbels -- Der WOCE-Schnitt A2. Berichte des BSH, No. 22, 156 pp.
- Luksch, U., 1996: Simulation of North Atlantic low-frequency SST variability. *Journal of Climate*, **9**, 2083-2092.
- Marotzke, J., 1997: Boundary mixing and the dynamics of three-dimensional thermohaline circulations. *J. Phys. Oceanogr.*, **27**, 1713-1728.
- Marsh, R., 2000: Recent Variability of the North Atlantic thermohaline circulation inferred from surface heat and freshwater fluxes. *Journal of Climate*, **13**, 3239-3260.
- Marshall, J., A.J.G. Nurser, and R.G. Williams, 1993: Inferring the subduction rate and period over the North Atlantic. *J. Phys. Oceanogr.*, **23**, 1315-1329.
- Marshall, J., H. Johnson, and J. Goodman, 2001a: A study of the interaction of the North Atlantic Oscillation with the ocean circulation. *Journal of Climate*, **14**, 1399-1421.
- Marshall, J., Y. Kushnir, D. Battisti, P. Chang, A. Czaja, R. Dickson, J. Hurrell, M. McCartney, R. Saravanan and M. Visbeck, 2001b: North Atlantic Climate Variability: phenomena, impacts and mechanisms. *Int. Journal of Climatology*, 21, 1863-1898.
- McLaughlin, F. A., E. C. Carmack, R. W. Macdonald and J. K. B. Bishop, 1996. Physical and geochemical properties across the Atlantic/Pacific water mass front in the southern Canadian Basin, *J. Geophys. Res.*, **101**, 1183-1197.
- Meincke, J., S. Jonsson and J. H. Swift. 1992. Variability of convective conditions in the Greenland Sea. *ICES mar. Sci. Symp.* **195**, 32-39.
- Meincke, J. and B. Rudels. 1995. Greenland Sea Deep Water: A balance between convection and advection. Nordic Seas Symposium., Hamburg, March 1995. Extended Abstr. Vol., U. Hamburg, 143-148.
- Meincke, J., Rudels, B. and Friedrich, H. J. 1997. The Arctic Ocean - Nordic Seas Thermohaline System. *J. Mar Sci.*, **54**, 283-299.
- Molinari, R. L., D. Mayer, J. F. Festa and H. F. Bezdek, 1997: Multiyear variability in the near-surface temperature structure of the midlatitude western North Atlantic Ocean. *J. Geophys. Res.*, **102**, 3267-3278.

- Molinari, R.L., R.A. Fine, W.D. Wilson, R.G. Curry, J. Abell and M.S. McCartney, 1998: The arrival of recently formed Labrador Sea Water in the Deep Western Boundary Current at 26.5N. *Geophys. Res. Lett.*, **25**: 2249-2252.
- Morison, J., M. Steele and R. Anderson, 1998a. Hydrography of the upper Arctic Ocean measured from the Nuclear Submarine, USS PARGO. *Deep-Sea Res.*, I **45** (1) 15-38.
- Morison, J, K. Aagaard, and M. Steele, 1998b. Report on the Study of the Arctic Change Workshop, November 10-12, 1997, Univ. of Washington, ARCSS Rept No. 8. 63 pp.
- Morison, J, K. Aagaard, and M. Steele, in press. Recent changes in the Arctic: a review. *Arctic*.
- Mork, K. A., and J. Blindheim, 2000. Variations in the Atlantic inflow to the Nordic Seas, 1955-1996. *Deep-Sea Res.*, I **47**. 1035-1057.
- Mysterud, A., N. C. Stenseth, N. G. Yoccoz, G. Ottersen, R. Langvatn: The Response of Terrestrial Ecosystems to Climate Variability Associated with the North Atlantic Oscillation, this volume.
- Orvik, K. A., O. Skagseth and M. Mork, 2001. Atlantic inflow to the Nordic Seas: current structure and volume fluxes from moored current meters, VM-ADCP and SeaSoar - CTD observations, 1995-1999. *Deep-Sea Res.*, I **48**, 937-957.
- Østerhus, S. and T. Gammelsrod, 1999. The Abyss of the Nordic Seas is Warming. *J. Clim.* **12**, 11: 3297-3304.
- Oschlies, A., 2001. NAO-induced long-term changes in nutrient supply to the surface waters of the North Atlantic. *Geophys. Res. Lett.*, **28**, 1751-1754.
- Paiva, A. M., and E. P. Chassignet, 2002: North Atlantic modeling of low-frequency variability in mode water formation. *J. Phys. Oceanogr.*, , in press.
- Parilla, G., A. Lavin, H. Bryden, M. Garcia and R. Millard, 1994: Rising temperatures in the subtropical North Atlantic Ocean over the past 35 years. *Nature*, **369**: 48-51.
- Parsons, A.T., 1969: Two layer model of Gulf Stream separation. *J. Fluid Mech.*, **39**: 511-528.
- Petrie, B. and K. Drinkwater, 1993: Temperature and salinity variability on the Scotian Shelf and in the Gulf of Maine 1945-1990. *J. Geophys. Res.*, **98**: 20079-20089.
- Quadfasel, D., A.Sy, D.Wells, and A.Tunik, 1991. Warming in the Arctic. *Nature*, **350**, 385.
- Rahmstorf, S. and A.Ganopolski, 1999. Long-term global warming scenarios computed with an efficient coupled climate model. *Climatic Change*, **43**, 353-367.
- Rahmstorf, S., 2001: A simple model of seasonal open-ocean convection. Part I: Theory. *Ocean Dyn.*, **52**, 26-35.
- Reverdin, G., D. Cayan, and Y. Kushnir, 1997: Decadal variability of hydrography in the upper northern North Atlantic in 1948-1990. *J. Geophys. Res.*, **102**: 8505-8531.

- Reverdin, G., N. Verbrugge, H. Valdimarsson, 1999: Upper ocean variability between Iceland and Newfoundland 1993-1998. *J. Geophys. Res.*, **104**, 29599-29611.
- Rodwell, M. J., On the predictability of the North Atlantic Climate, this volume.
- Rogers, J. C., 1990: Patterns of low-frequency monthly sea-level pressure variability (1899-1986) and associated wave cyclonic frequencies. *J. Climate*, **3**, 1364-1379.
- Rudels, B. and D. Quadfasel. 1991. Convection and deep water formation in the Arctic Ocean-Greenland Sea system. *J. Mar. Sys.* **2** (3/4), 435-450.
- Saravanan, R., and J. C. McWilliams, 1998: Advective ocean-atmosphere interaction: an analytical stochastic model with implications for decadal variability. *J. Climate*, **11**, 165-188.
- Schlosser, P., G. Bonisch, M. Rhein and R. Bayer. 1991. Reduction of deepwater formation in the Greenland Sea during the 1980's: Evidence from tracer data. *Science*, **251**, 1054-1056.
- Seager, R., Y. Kushnir, M. Visbeck, N. Naik, J. Miller, G. Krahnmann and H. Cullen, Causes of Atlantic Ocean climate variability between 1958 and 1998, *J. Climate*, **13**, 2845-2862, 2000.
- Selten, F. M., R. J. Haarsma and J. D. Opsteegh, 1999: On the mechanism of North Atlantic Decadal Variability. *J. Climate*, **12**, 1956-1973.
- Smethie, W.M., R.A. Fine, A. Putzka and E.P.Jones, 2000: Tracing the flow of North Atlantic Deep Water using chlorofluorocarbons. *J. Geophys. Res.*, **105**: 14297-14323.
- Stephenson, D.B., H. Wanner, S. Brönnimann, J. Luterbacher, The History of Scientific Research on the North Atlantic Oscillation, this volume
- Sturges, W., and B.G. Hong, Wind forcing of the Atlantic thermocline along 32°N at low frequencies, *J. Phys. Oceanogr.*, **25**, 1706-1715, 1995.
- Straile, D., D.M. Livingstone, G.A. Weyhenmeyer, and D.G. George: The Response of Freshwater Ecosystems to Climate Variability Associated with the North Atlantic Oscillation, this volume.
- Sutton, R. T., and M. R. Allen, 1997: Decadal predictability of North Atlantic sea surface temperature and climate. *Nature*, **388**, 563-567.
- Swift, J. H., E. P. Jones, K. Aagaard, E. C. Carmack, M. Hingston, R. W. Macdonald, F. A. McLaughlin, and R. G. Perkin. 1997. Waters of the Makarov and Canada Basins, *Deep-Sea Res.*, **44** (8), 1503-1529.
- Sy, A., M. Rhein, J. R. N. Lazier, K. P. Koltermann, J. Meincke, A. Putzka, and M. Bersch, 1997: Surprisingly rapid spreading of newly formed intermediate waters across the North Atlantic Ocean. *Nature*, **386**, 675-679.
- Talley, L. D. and M. E. Raymer, 1982: Eighteen degree water variability. *J. Mar. Res.*, **40** (S), 757-775.
- Talley, L. E., 1996, North Atlantic circulation and variability, reviewed for the CNLS conference. *Physica D*, **98**, 625-646.

- Taylor, A.H., and A. Gangopadhyay, 2001. A Simple Model of Interannual Shifts of the Gulf Stream, *J. Geophys. Res.*, **106**, 13,849-13,860.
- Taylor, A.H. and J.A. Stephens, 1998. The North Atlantic Oscillation and the latitude of the Gulf Stream. *Tellus*, **50**,134-142.
- Tereshchenko, V.V., 1996. Seasonal and year-to-year variations of temperature and salinity along the Kola meridian transect. ICES CM 1996/C:11 24 pp (mimeo).
- Thompson, D.W.J., S. Lee, and M.P. Baldwin: Atmospheric Processes Governing the Northern Hemisphere Annular Mode/North Atlantic Oscillation, this volume.
- Turrell, W. R., G. Slessor, R. D. Adams, R. Payne and P. A. Gillibrand. 1999. Decadal variability in the composition of Faroe-Shetland Channel bottom water. *Deep-Sea Res.*, I 46, 1-25.
- Verduin, J. and D. Quadfasel 1999. Long-term temperature and salinity trends in the central Greenland Sea. In: E. Jansen (ed.) European Sub-Polar Ocean Programme II, Final Scientific Report.
- Veronis, G., 1973: Model of World Ocean Circulation: I. Wind-driven, two-layer. *J. Mar. Res.*, 31, 228-288.
- Vinje, T., N. Nordlund, and A. Kvambekk, 1998: Monitoring ice thickness in Fram Strait. *J. Geophys. Res.*, **103**, 10437-10449.
- Vinje, T., 2001a: Anomalies and Trends of Sea-Ice Extent and Atmospheric Circulation in the Nordic Seas during the Period 1864-1998. *J. Climate.*, **14**, 255-267.
- Vinje, T., 2001b. Fram Strait ice fluxes and atmospheric circulation, 1950-2000. *J. Climate*, **14** 3508-3517.
- Visbeck, M., H. Cullen, G. Krahnmann and N. Naik, 1998: An oceans model's response to North Atlantic Oscillation like wind forcing. *Geophys. Res. Lett.*, **25**, 4521-4524.
- Visbeck, M., J. Hurrell, L. Polvani and H. Cullen, 2001: The North Atlantic Oscillation, Present, Past and Future., *PNAS*, **98**, 12876-12877.
- Visbeck M. and M. Rhein, 2000. Is bottom boundary layer mixing slowly ventilating Greenland Sea Deep Water? *J. Phys. Oceanogr.*, **30**, 215-224.
- Yang, J.,1999: A linkage between decadal climate variations in the Labrador Sea and the tropical Atlantic Ocean. *Geophys. Res. Letters*, **26**,1023-1026.
- Wallace, J. M., and D. S. Gutzler, 1981: Teleconnections in the geopotential height field during the Northern Hemisphere winter. *Mon. Wea. Rev.*, **109**, 784-812.
- Walker, G.T. and Bliss, E. W., 1932: World Weather V. *Mem. R. Meteorol. Soc.*, **44**, 53-83.
- Watanabe, M. and M. Kimoto, 2000: On the Persistence of Decadal SST Anomalies in the North Atlantic. *Journal of Climate* , **13**, 3017-3028.

Weng, W., and J. D. Neelin, 1998: On the role of ocean-atmosphere interaction in midlatitude interdecadal variability. *Geophysical Research Letters*, **25**, 167-170.

Woodruff, S.D., R.J. Slutz, R.L. Jenne, and P. M. Streurer, 1987: A comprehensive ocean-atmosphere data set. *Bull. Amer. Meteor. Soc.*, **68**, 1239-1250.

Xie, S.-P. and Y. Tanimoto, 1998: A pan-Atlantic decadal climate oscillation. *Geophysical Research Letters*, **25**, 2185-2188.

Zhang, J., D. Rothrock, and M. Steele, 2000: Recent changes in Arctic sea ice: The interplay between ice dynamics and thermodynamics, *J. Climate*, **13**, 3099-3114.

Table1:

Property	High NAO index phase	Remarks
SLP subtropical High	Stronger subtropical High (+ 3-5 HPa)	
SLP Icelandic Low	Deeper polar Low (- 7-9 HPa)	
Storm tracks	More northeasterly tilted and extended tracks	
Heat flux over subpolar gyre	Enhanced ocean heat loss by 20-50 W m ⁻²	
Heat flux over subtropical gyre	Reduced ocean heat loss by 15-35 W m ⁻²	
SST within subpolar gyre	0.5-1.0 °C colder	For interannual up to decadal periods.
SST western subtropical gyre	0.3-0.7 °C warmer	
SST northeastern tropical Atlantic	0.4-0.8 °C colder	
Gulf Stream position	20-50 km north of its mean position (~39°N) between 70-60°W	[Joyce et al. 2000]
Baroclinic transport (Labrador Sea - Bermuda)	Enhanced eastward transport between the gyre by 5-9 Sv	[Curry and McCartney 2001]
Thickness change of Labrador Sea Water	50-100 m increase per year of forcing	[Curry et al. 1998]
Transport of Florida Current	Reduced by 1-2 Sv out of a mean of 32 Sv	[Baringer and Larsen, 2001]
Ice cover in Labrador Sea	Enhanced	[Deser et al. 2000]
Ice cover in Greenland Sea	Reduced	[Deser et al. 2000]
Deep mixing (convection) in the Labrador Sea	Enhanced up to 2500m maximum depth	[Dickson et al. 1996; Lazier 1995]

Figure Captions:

Figure 1: Left: Regression/covariance of the Kaplan et al. [1997, 1998; <http://ingrid.ldeo.columbia.edu/SOURCES/.KAPLAN/.EXTENDED>] reconstructed SST data set with the Hurrell [1995; <http://www.cgd.ucar.edu/~jhurrell/nao.html>] normalized NAO index, both averaged over the winter (December-March) season from 1900-2000. Positive values are shown with solid contours, negative values with dashed contours, and zero regression is represented by a dotted line. Note, that a strong NAO winter season will have about twice the temperature anomaly given in the plot. When shorter SST records from other data sets have been used the SST covariance tends to be somewhat larger. However, pattern and correlation magnitudes are similar. Right: same as left but correlation is shown. Maximum values are on the order of 0.3-0.5, which means that the NAO explains only 8-20% of the total winter SST variance.

Figure 2: Lag correlation between the Kaplan et al. [1997, 1998] SST anomalies and the Hurrell [1995] winter NAO index. Negative lags (top row) have the ocean leading the atmospheric pressure, bottom row shows the ocean responding to changes in the atmospheric forcing. Correlation above 95% significance are hatched. Positive values are shown with solid contours, negative values with dashed contours, and zero correlation is represented by the dotted line. Note that the maximum correlation is found when SST lags the NAO index by 0-2 years. The normalized NAO index is given in the middle for reference.

Figure 3: The upper left graph shows the covariance between the NAO-index and the NCEP/NCAR reanalysis wind stress on the ocean. The maximum response is found at 50°N with enhanced westerly wind stress by 0.1 N m^{-2} . The upper right graph shows the correlation coefficient between NAO-index zonal wind stress and NAO-index with maximum values of 0.8. The lower left graph shows the covariance between wind speed and NAO-index showing enhanced wind speed over the subpolar gyre and in the tropical North Atlantic. The lower right graph shows the barotropic equilibrium stream function anomaly as predicted from the wind stress curl using Sverdrup theory (see text for details). We expect an enhanced anticyclonic wind driven circulation of 6 Sv located between the subtropical and subpolar gyre (the 'inter-gyre gyre').

Figure 4: The graph shows the covariance between NAO-index and the NCEP/NCAR reanalysis (1958-2000) latent heat flux (top left) and the sensible heat flux (top right). Changes in the Ekman transport (bottom right) alter the upper ocean heat transport and its divergence is expressed here as a surface heat flux (bottom left). The solid lines in the lower right graph show the climatological winter SSTs and the arrow represent the NAO induced surface Ekman transport.

Figure 5: The top left graph shows the covariance between the NAO-index and the NCEP/NCAR reanalysis precipitation multiplied by -1. The top right graph shows the covariance between the NAO-index and NCEP/NCAR reanalysis evaporation. The bottom left graph shows how changes in the surface Ekman transport acting on the mean salinity gradient will effect the surface fresh water balanced (expressed here as a fresh water flux anomaly). The bottom right graph shows the sum of all fresh water fluxes. In most regions, precipitation and in particular the Ekman induced fresh water flux anomalies dominate the net surface fresh water flux.

Figure 6: This graph shows several zonally averaged fluxes regressed on the winter NAO index using fields from the NCEP/NCAR reanalysis data set. Part a) shows latent and sensible heat

fluxes and their sum, as well as the apparent heat flux caused by the wind driven Ekman transport divergence (see Figure 4). Part b) combines the zonally averaged precipitation and evaporation and their difference, as well as the apparent fresh water flux caused by the wind driven Ekman transport divergence (see Figure 5). Part c) shows the buoyancy flux caused by heat and freshwater fluxes and shows that it is dominated by the air-sea heat flux. Part d) shows the zonal component of the wind stress for reference. The horizontal lines at 62°N and 47°N denote the local extrema of the wind stress curl. We caution that in particular the fresh water fluxes might have significant errors associated with them.

Figure 7: a) Integrated air-sea flux anomalies from the NCEP/NCAR reanalysis starting from the equator towards the pole. Under the assumption that changes in ocean heat content are small (which is only true for very long time scales) this change would need to be balanced by similar changes in the ocean heat transport. b) Ocean heat transport anomaly caused by Ekman transport anomalies acting on the mean temperature gradient (see also Figure 4). For reference we also include the part that is caused by the mean Ekman transport divergence action on temperature anomalies (dashed line, and is quite a bit smaller compared to the other term). c) Ekman transport anomaly. d) Expected equilibrium boundary current transport anomaly using linear Sverdrup balance (might be expected on long time scales under idealized conditions; see also Figure 3).

Figure 8:

a) Time series of 0-2000 db potential energy at Bermuda (black circles) and smoothed with 3-point running mean (black curve) scale is left axis. Annual sea level anomaly (unsmoothed) is portrayed by the green curve and right axis scale. Florida Current transport from Baringer and Larsen [2001] is the red curve and red axis. b) Time series of 0-2000 db potential energy from the central Labrador Basin (black circles and curve, as above). Temperature at 1500 db, the LSW core, is depicted by the blue curve (unsmoothed annual values) and right axis scale. c) Index of eastward baroclinic mass transport between the subpolar and subtropical gyre centers (black curve is smoothed with 3-year running mean; black circles are annual values) from Curry and McCartney [2001]. The pink and blue bars depict Hurrell's SLP NAO index. The red dashed curve is the NAO index smoothed with a 3-point running mean. The solid red curve is the "integrated" NAO index from Curry and McCartney [2001] in which each point is evaluated as the weighted sum of the 10 previous years to simulate ocean "memory".

Figure 9: Subtropical temperature anomaly for the mid-depth layer 1500 - 2000 m near Bermuda. The broken line is the warming trend inferred by Joyce and Robbins [1996] who only used the data between 1955 and 1993.

Figure 10: Changes in the salinity (upper panel) and potential temperature (lower panel) of the water column in the Central Labrador Sea over the complete period of the hydrographic record since 1938. The data set was selected to lie within the 3300m isobath of the Labrador Sea, and the plots represent the median values of vertical property profiles, binned according to σ_{θ} density intervals. Figure was kindly provided by Igor Yashayaev, Bedford Institute of Oceanography, Dartmouth, N.S., Canada.

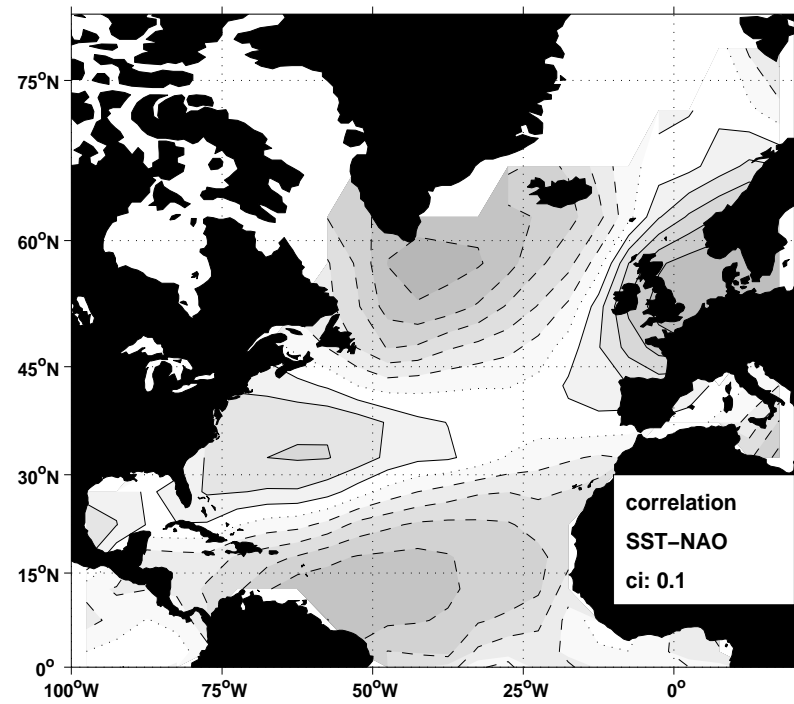
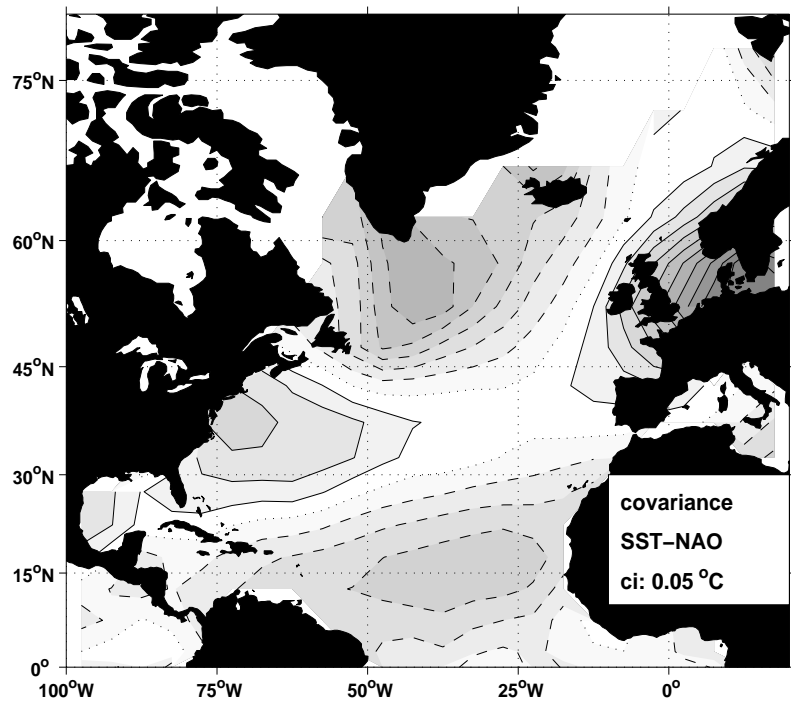
Figure 11: Change in the T-S relation between 1964-72 and 1995-97 for deep waters of the NW Atlantic (38-64 N, 12-52 W) denser than $\sigma_{\theta} = 36.84$ (LSW + NEADW + DSOW). Figure shows a volumetric T-S analysis kindly provided by Igor Yashayaev, Bedford Institute of Oceanography, Dartmouth, N.S., Canada. This remarkable change reflects the multi-decadal freshening of the entire system of overflow and entrainment that ventilates the deep Atlantic [Dickson et al 2002].

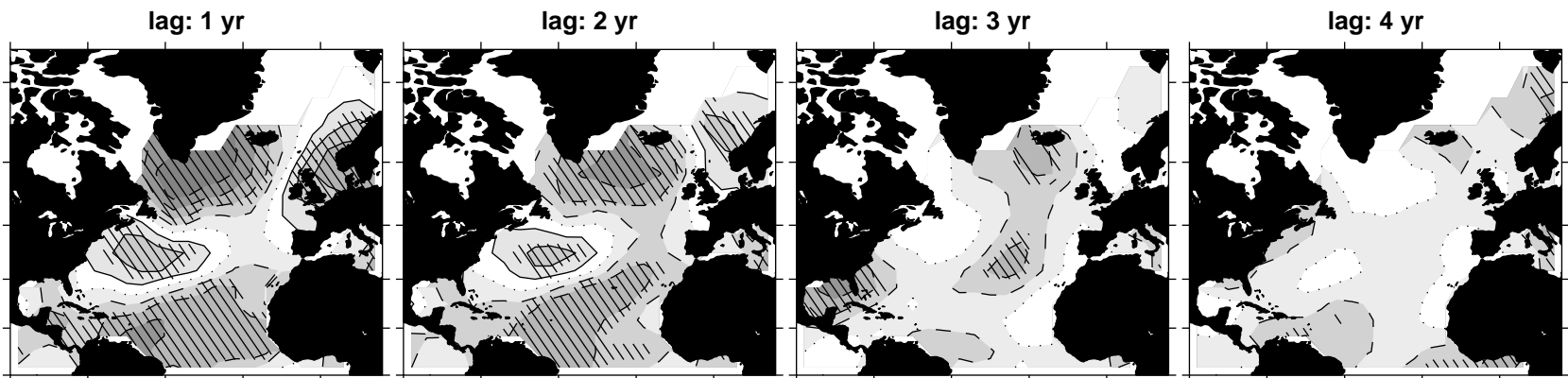
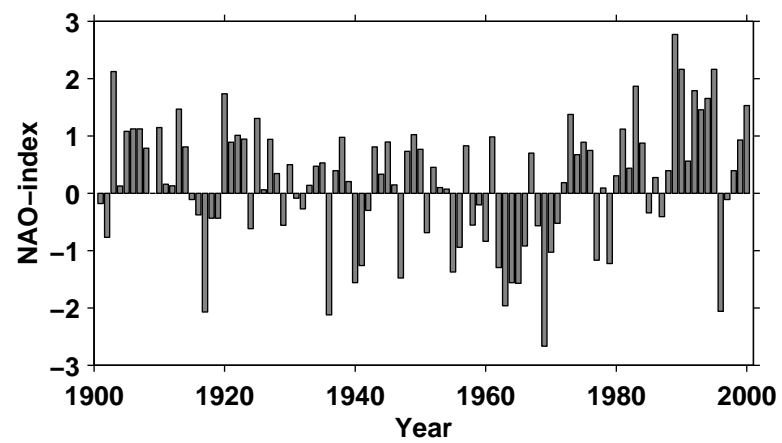
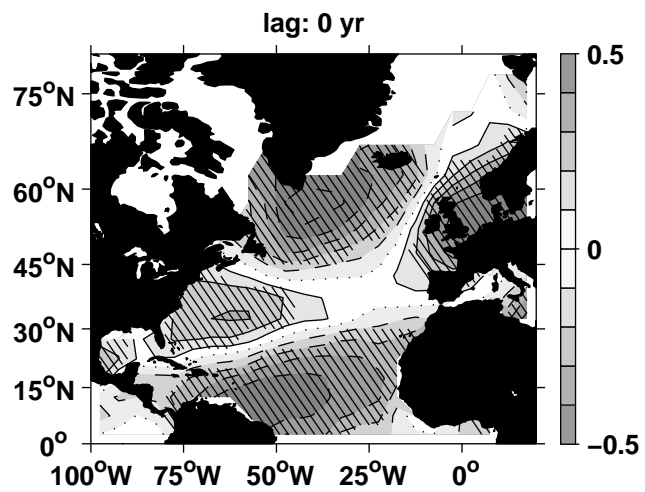
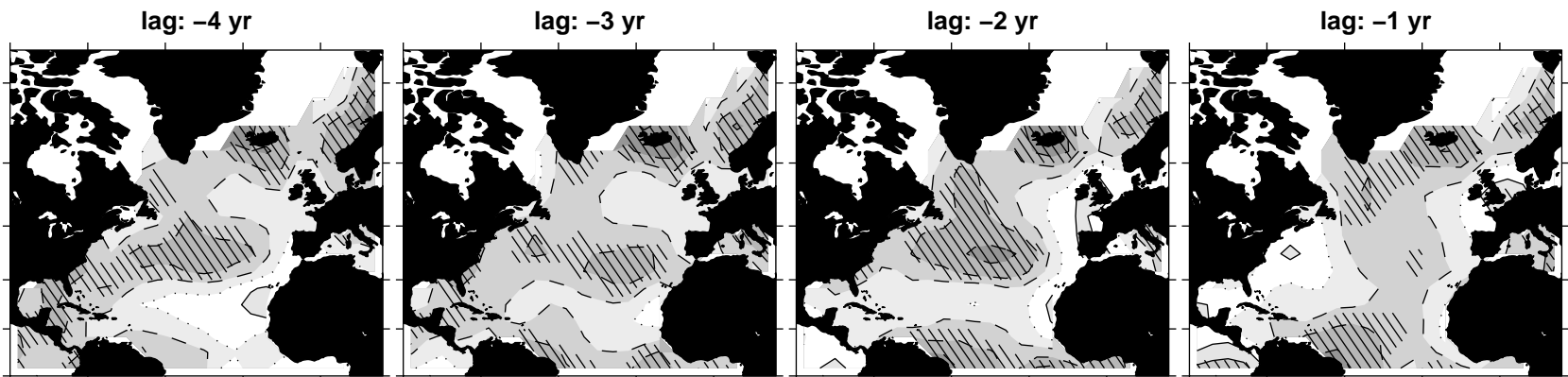
Figure 12: Winter (JFM) Arctic sea ice concentration from 1950 to 1995 (Chapman and Walsh, 1993) regressed onto the NAO index. Contoured are 3 and 6% changes in ice concentration. The arrows are the winter wind anomaly regressed onto the NAO index (see also Figure 3). The darker patches show increased ice concentration during a positive NAO while the lighter patches show the areas where ice concentration is reduced. The sea ice concentration response to the NAO shows a pronounced seesaw pattern between the Labrador and GIN Seas.

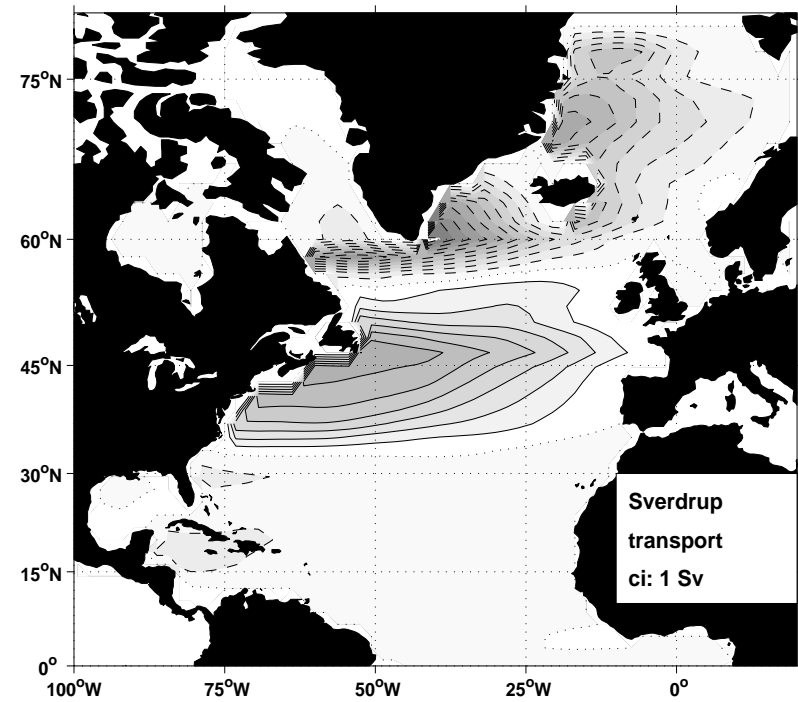
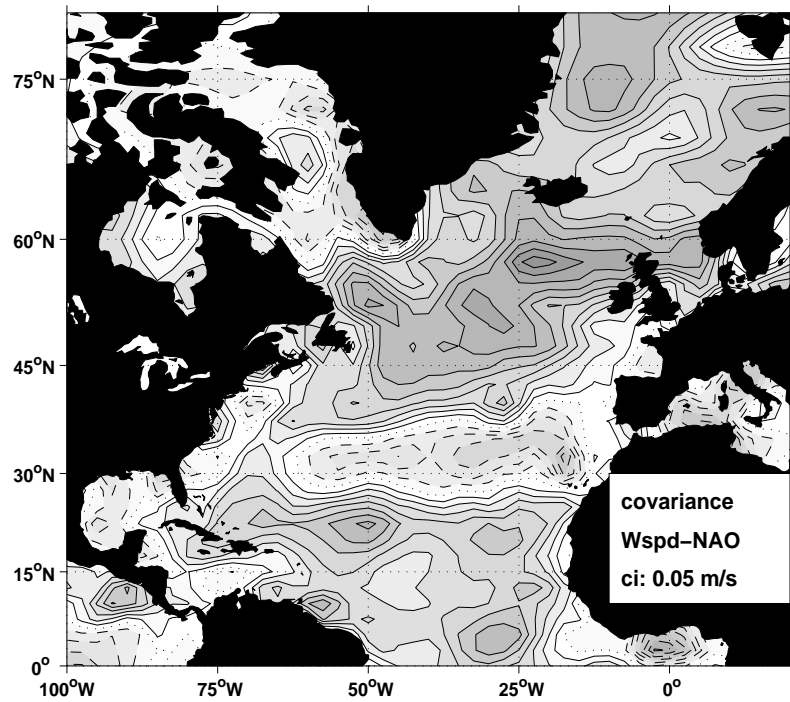
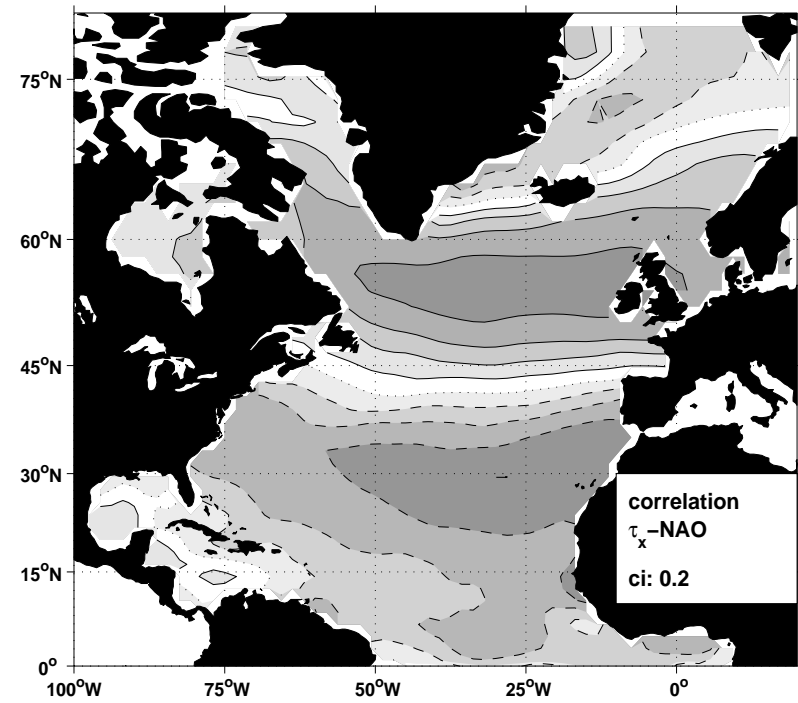
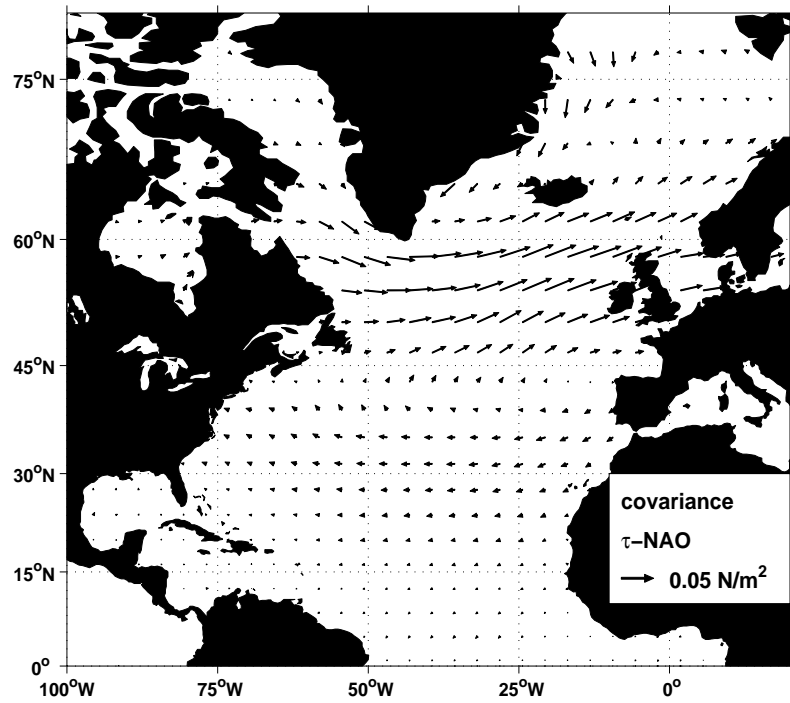
Figure 13: Time series of winter (JFM) sea ice concentration (Chapman and Walsh, 1993) area averaged for the Labrador Sea, Greenland Sea, and Barents Seas as well as the NAO index (lower panel). The heavy lines are obtained with a 5 year running mean filter. For each region the correlation coefficient with the NAO index is given and ranges from $r=0.35$ in the Labrador Sea to $r=-0.62$ in the Greenland Sea region.

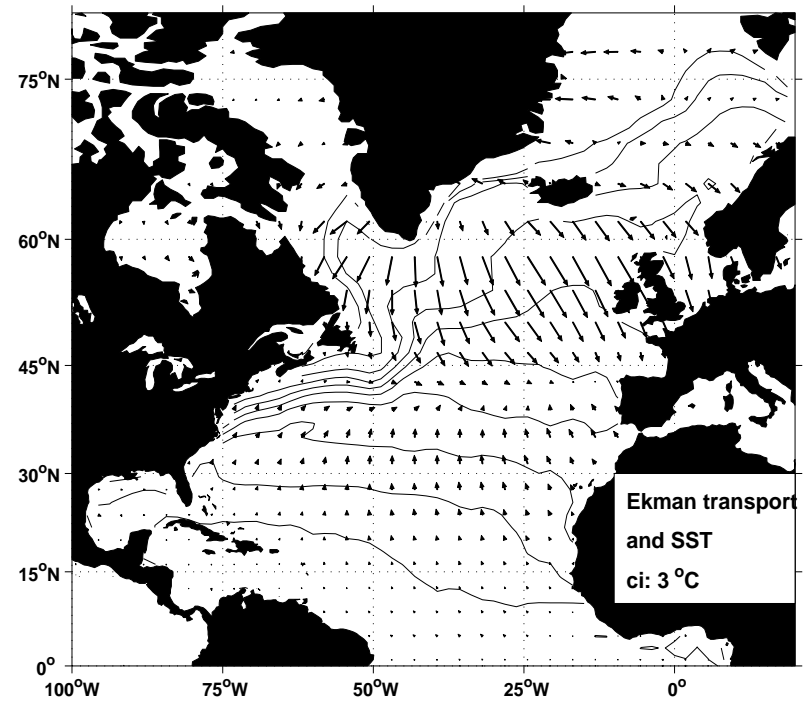
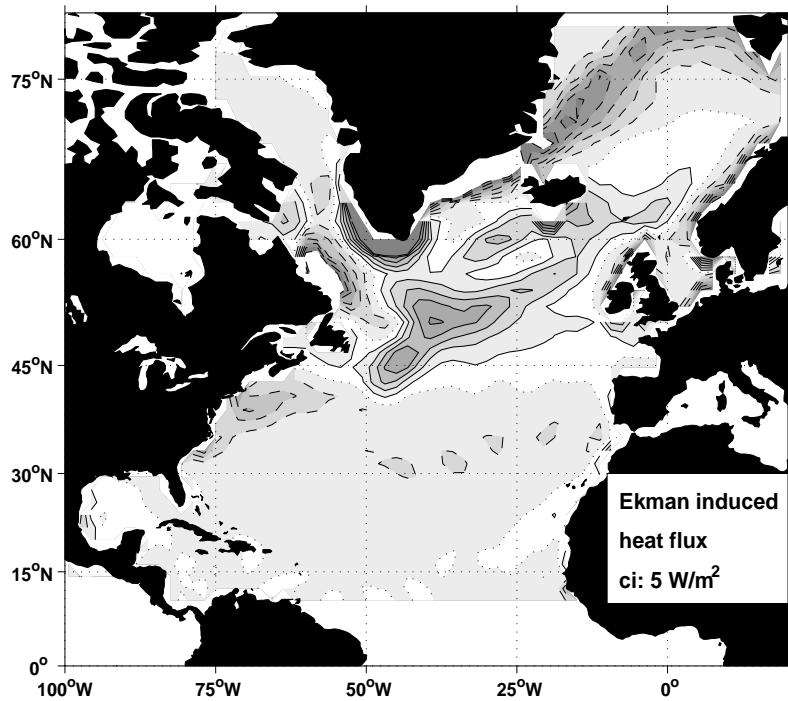
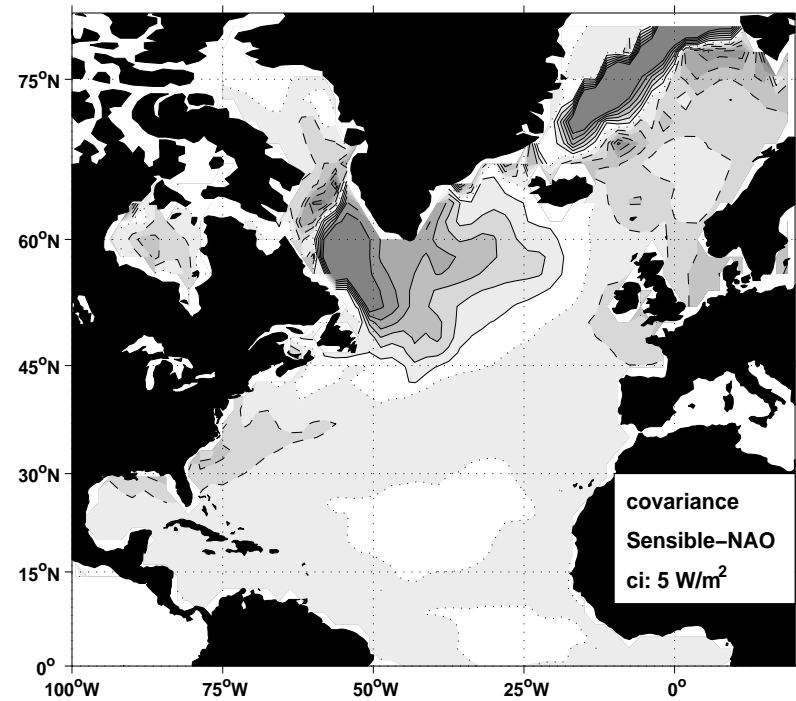
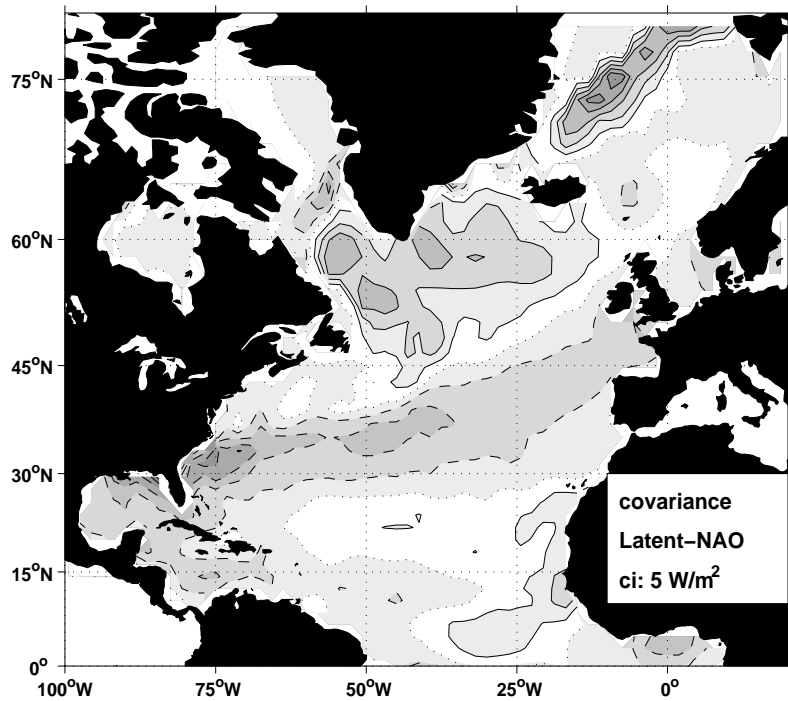
Figure 14: Correlation of Hurrell NAO index with Kaplan SST anomalies (left part) which is dominated by the interannual variability. Immediately to the right we present a schematic drawing of the zonally averaged Ekman induced meridional overturning circulation (MOC) in the ocean. Below that is a time series of the NAO index for reference.

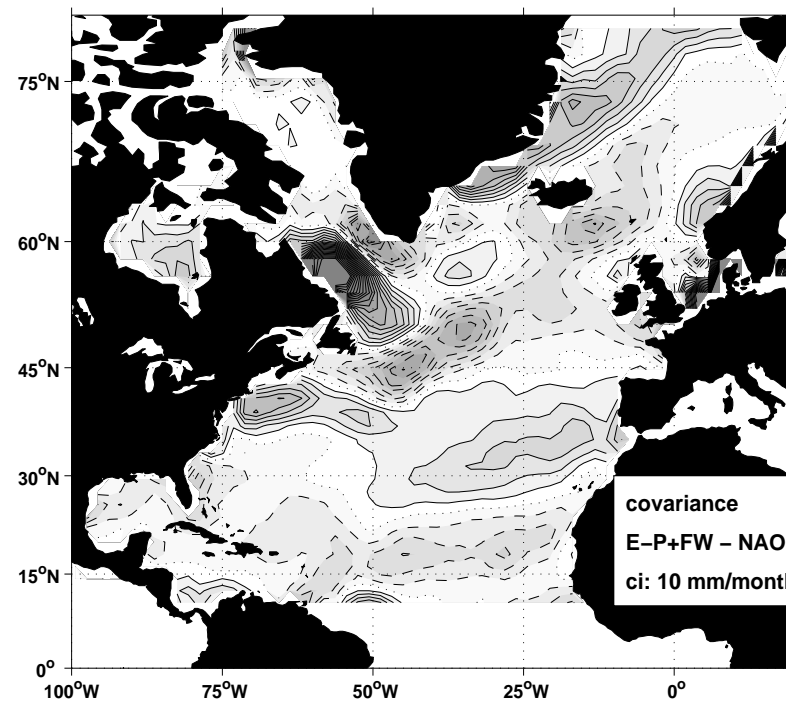
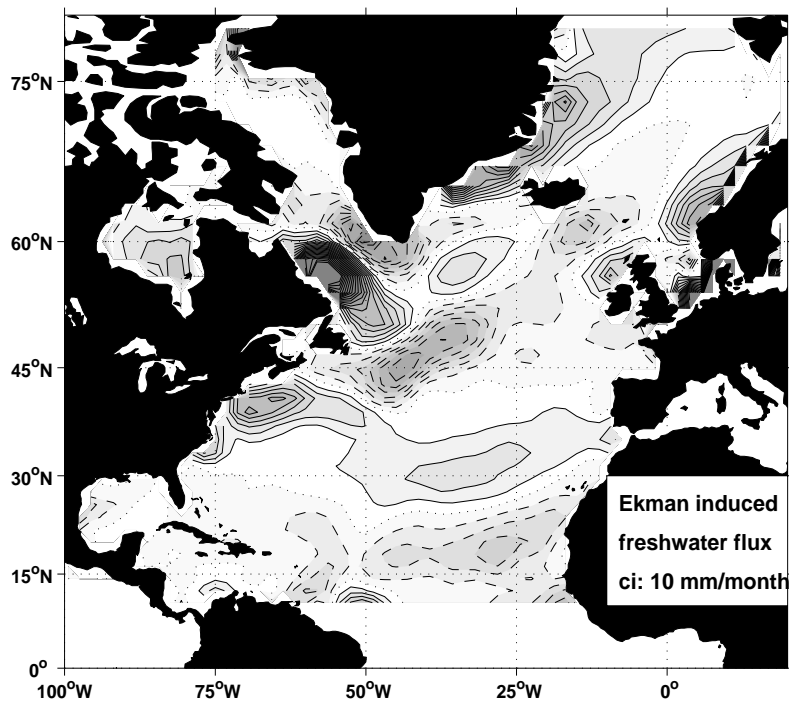
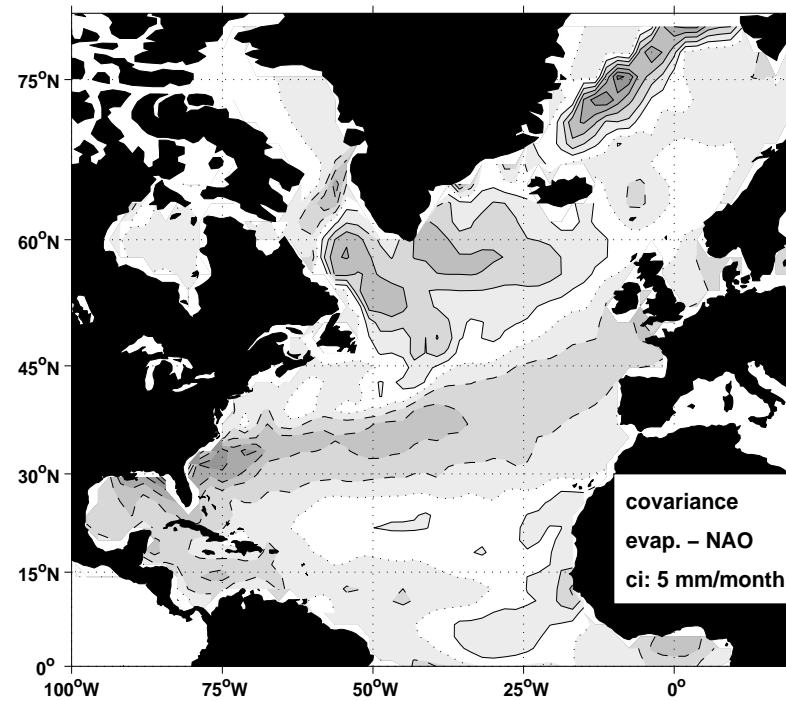
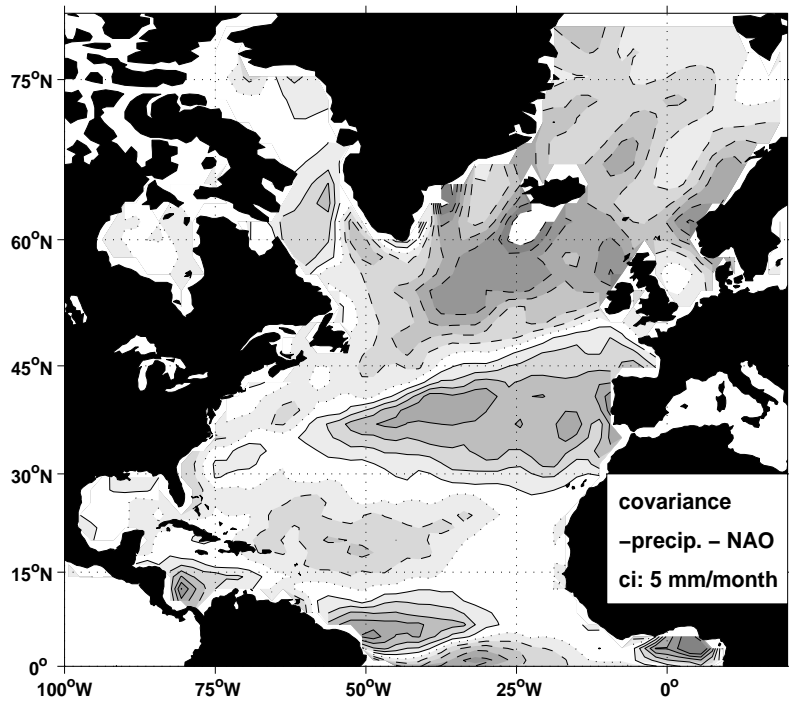
The right part of the figure shows the 6 year lag correlation (ocean lags atmosphere) between the 15 year low pass filtered NAO index (shown below) and the low pass filtered Kaplan SST anomalies. This part of the figure represents the decadal and lower frequency response of the ocean to NAO like forcing. Notice the down stream shift (arrows indicate position and strength of the Gulf Stream / North Atlantic Current) of the positive SST anomaly and the "loss" of the subpolar gyre cooling region. Model results have suggest that this switch could either be due to downstream dispersion of the warm temperature anomaly by the mean flow [Krahmann et al. 2001] or due to an increase in the Atlantic MOC [Eden and Willebrand, 2001] as indicated by the MOC schematic to the left.

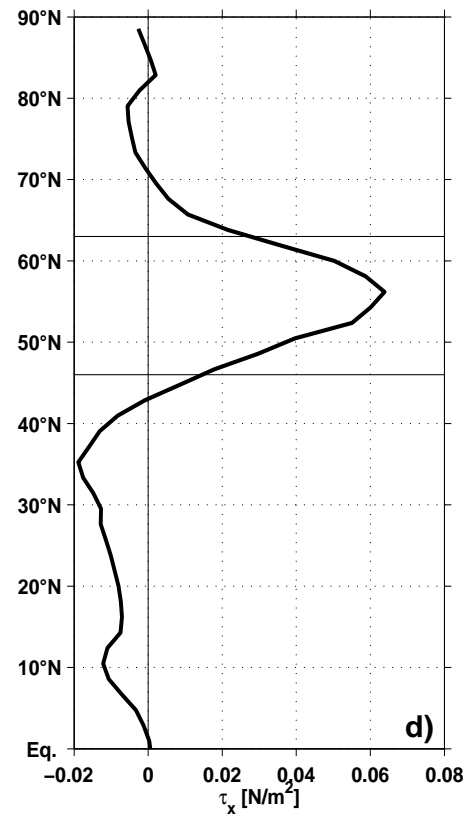
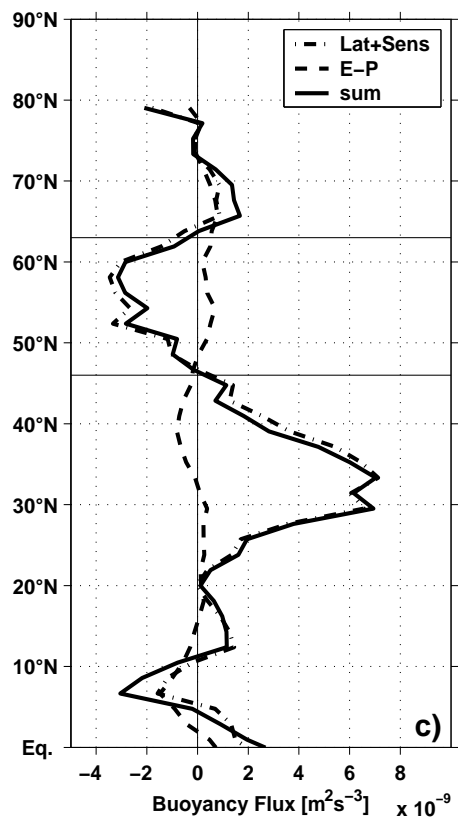
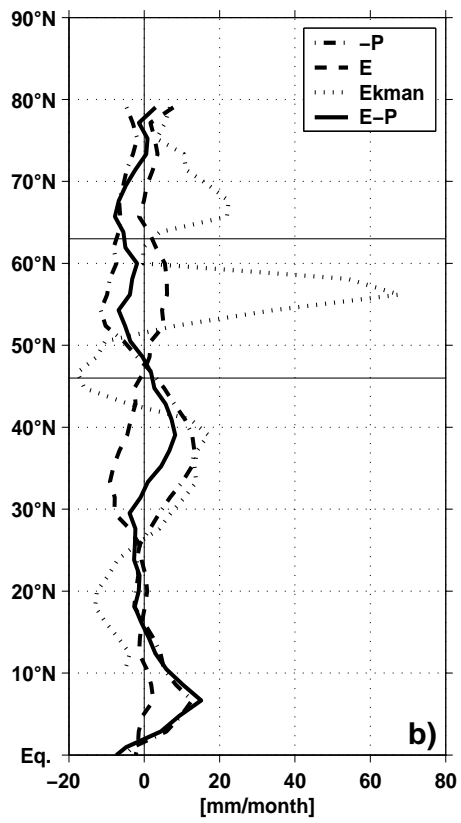
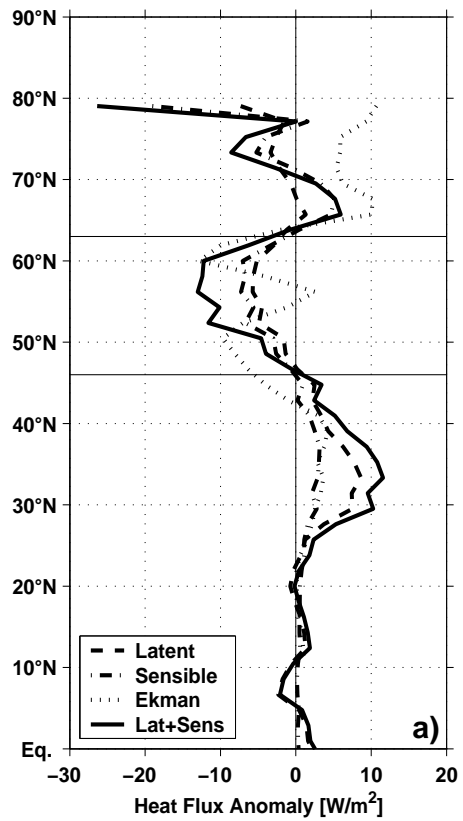


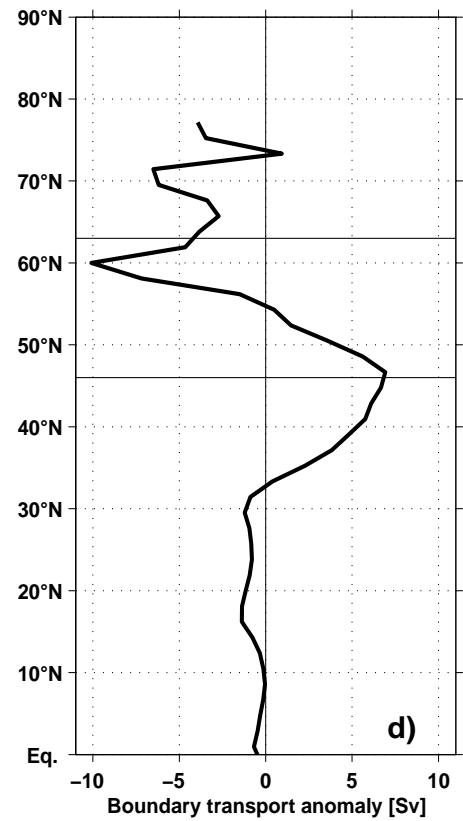
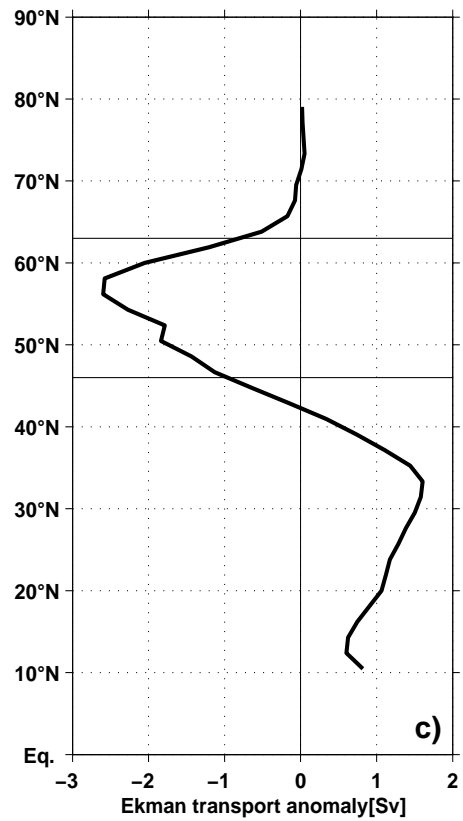
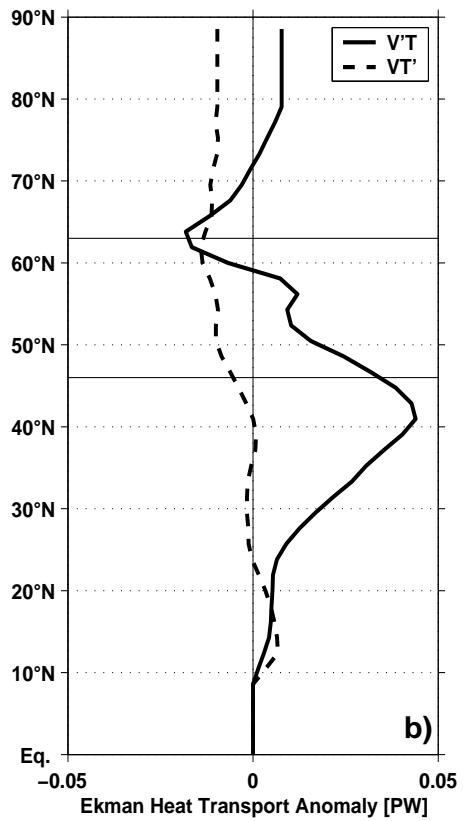
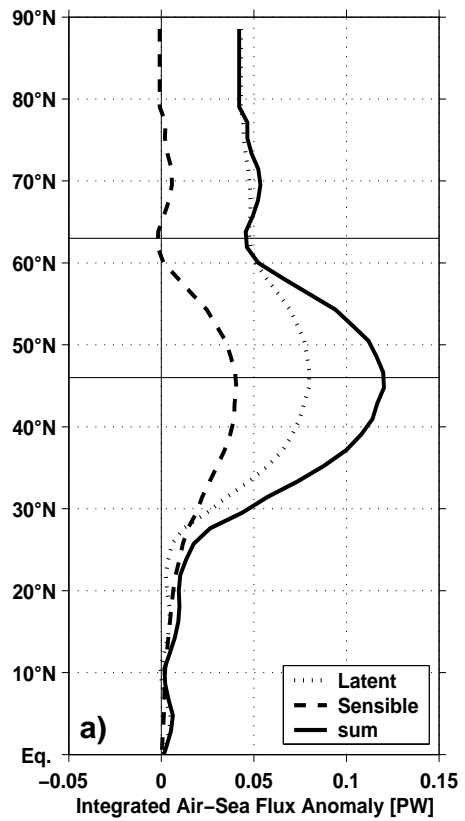


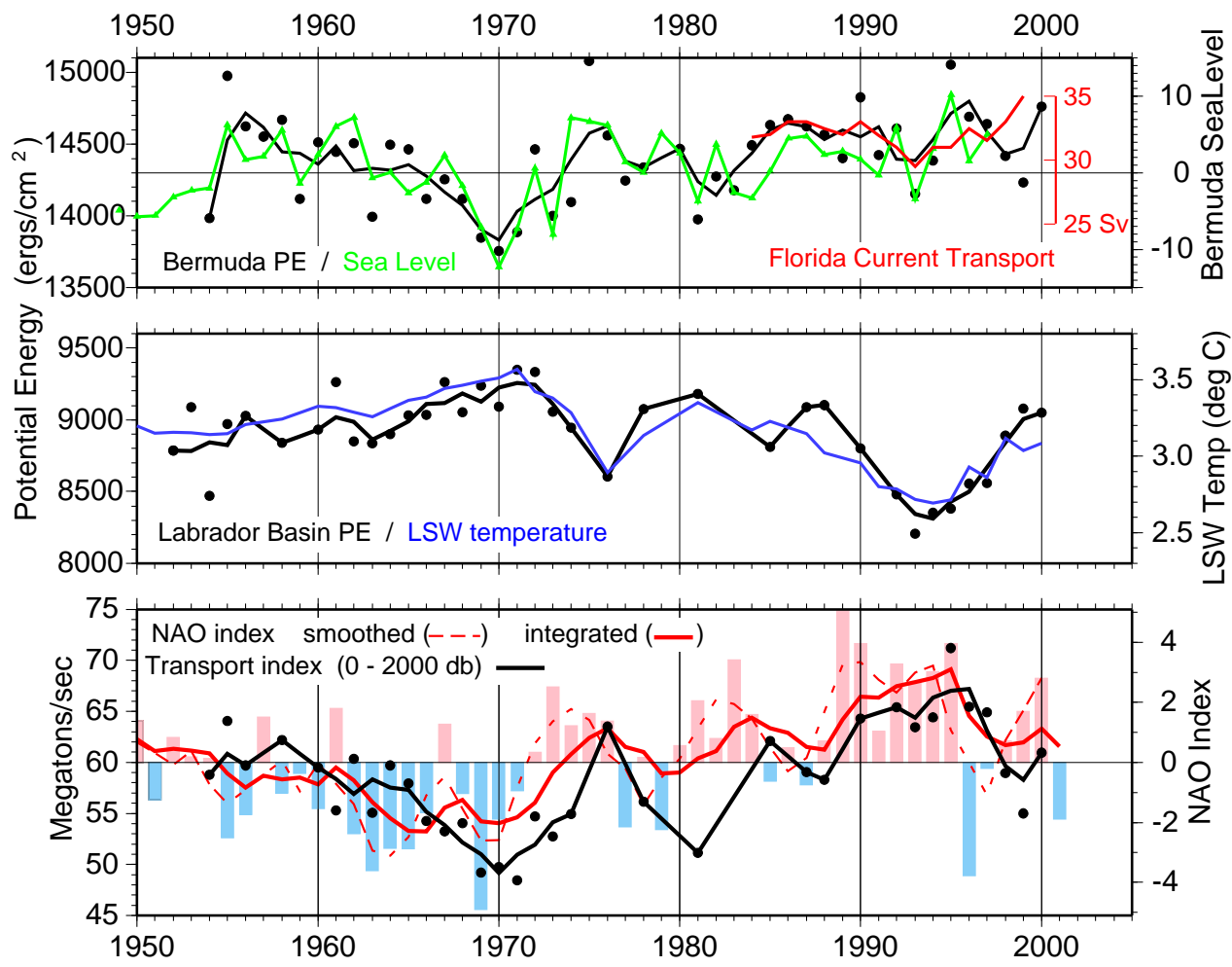


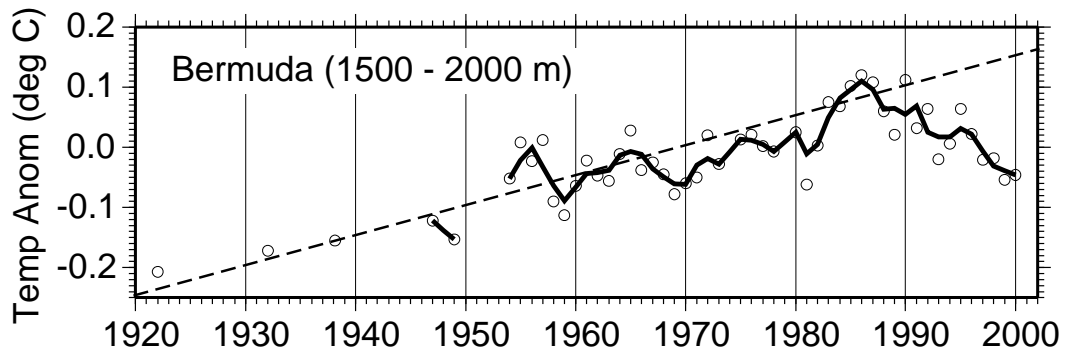


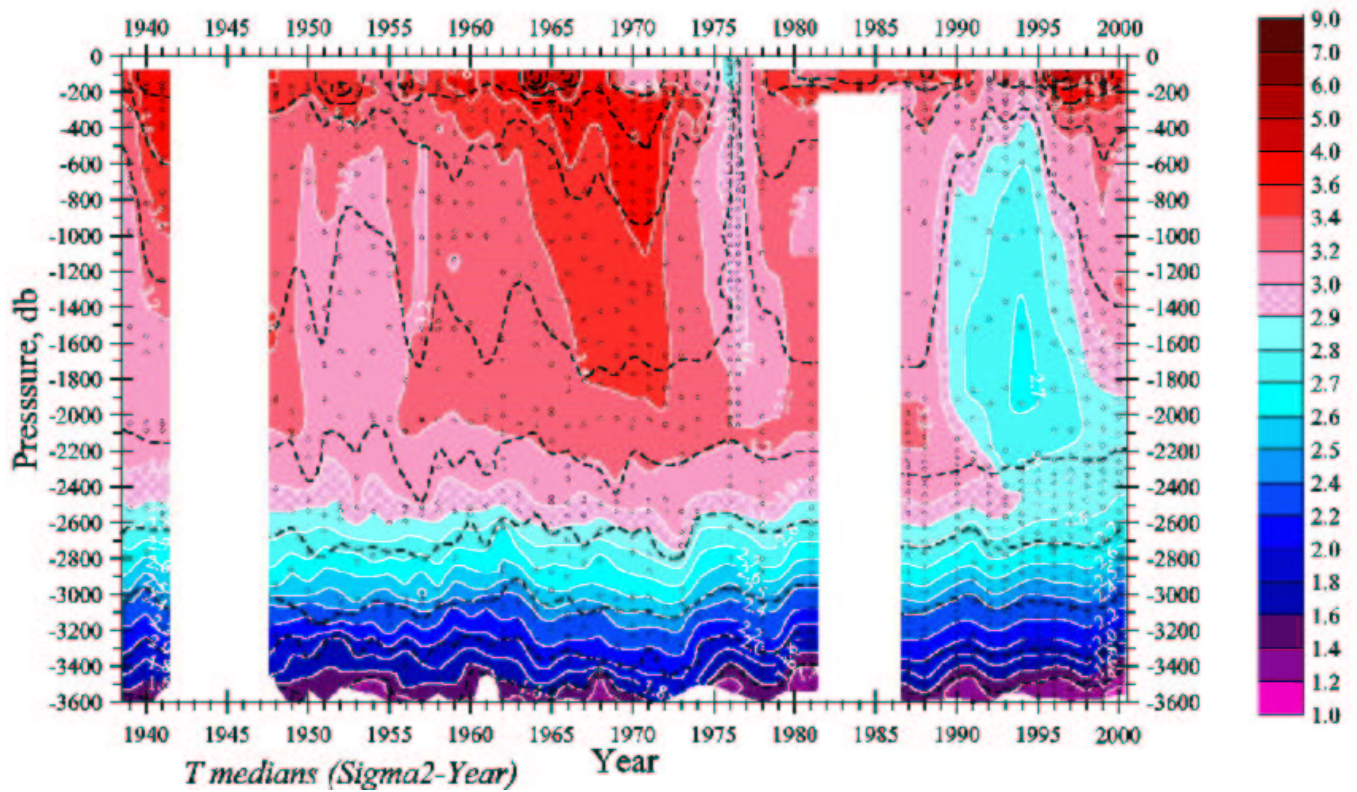
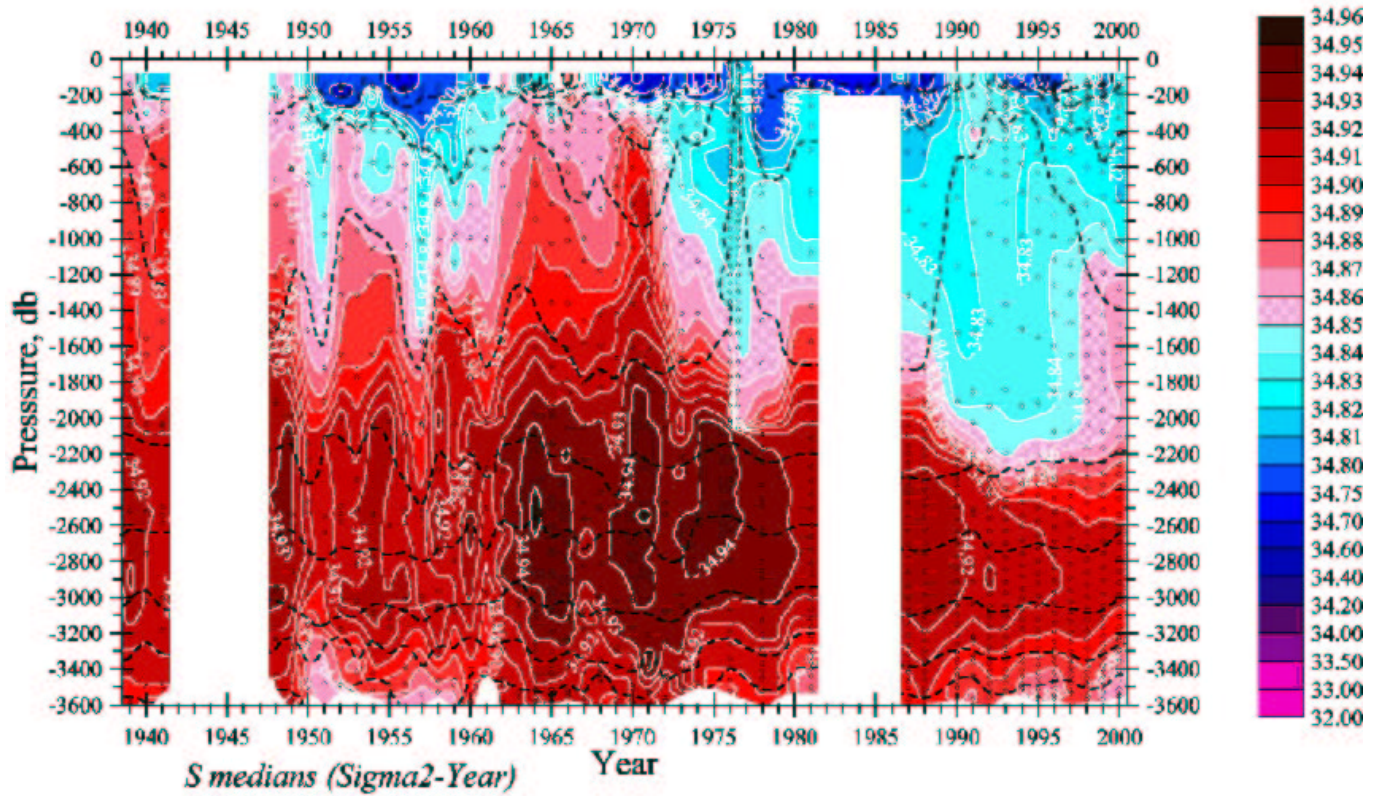




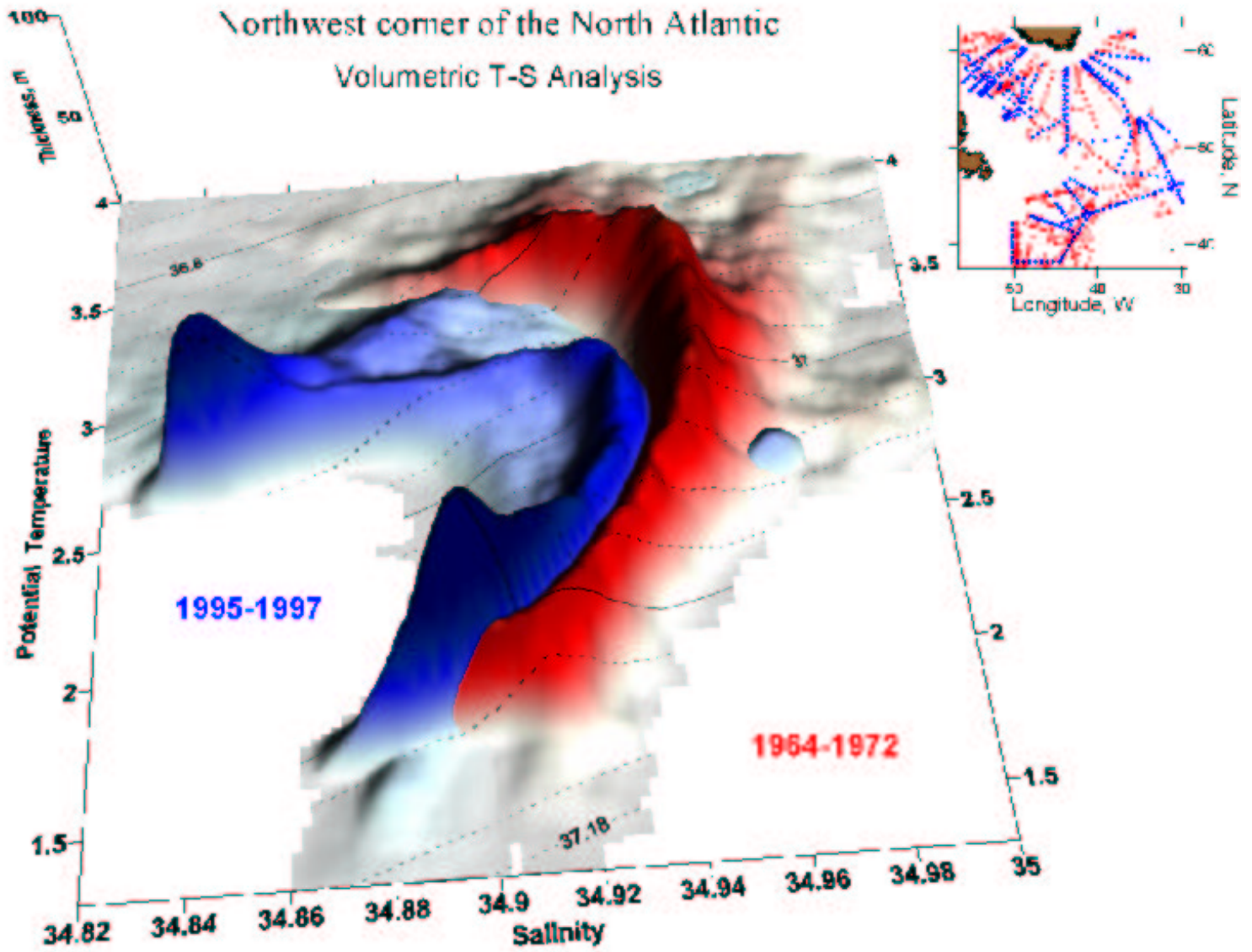


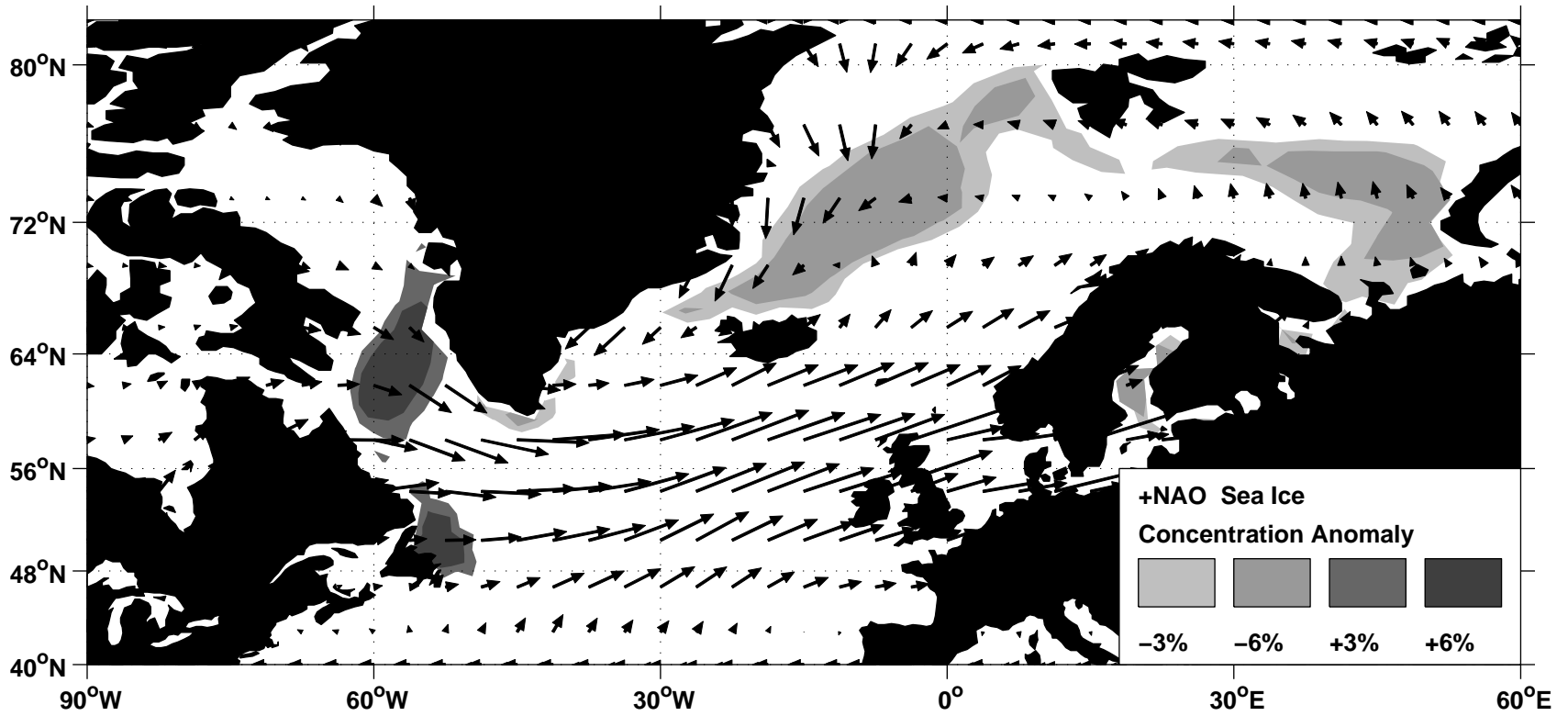




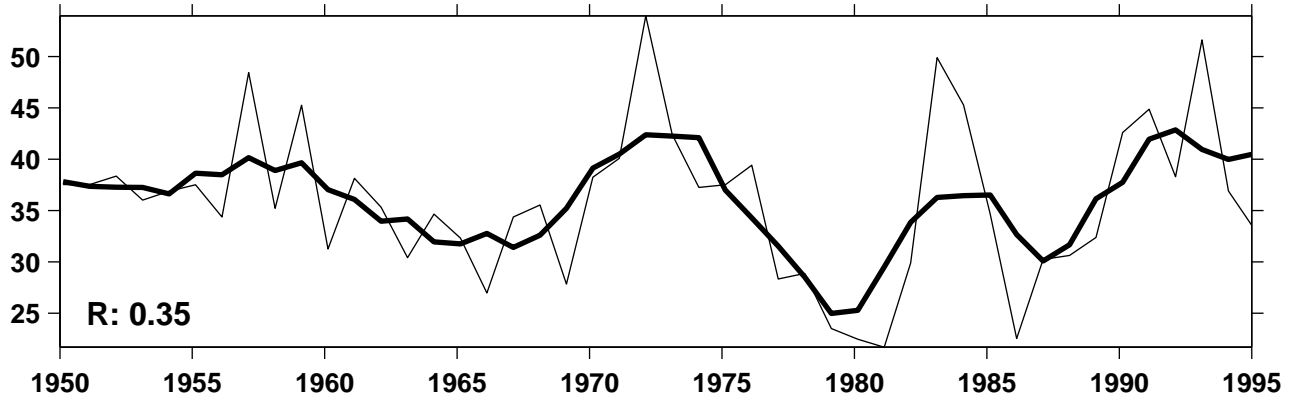


Northwest corner of the North Atlantic Volumetric T-S Analysis

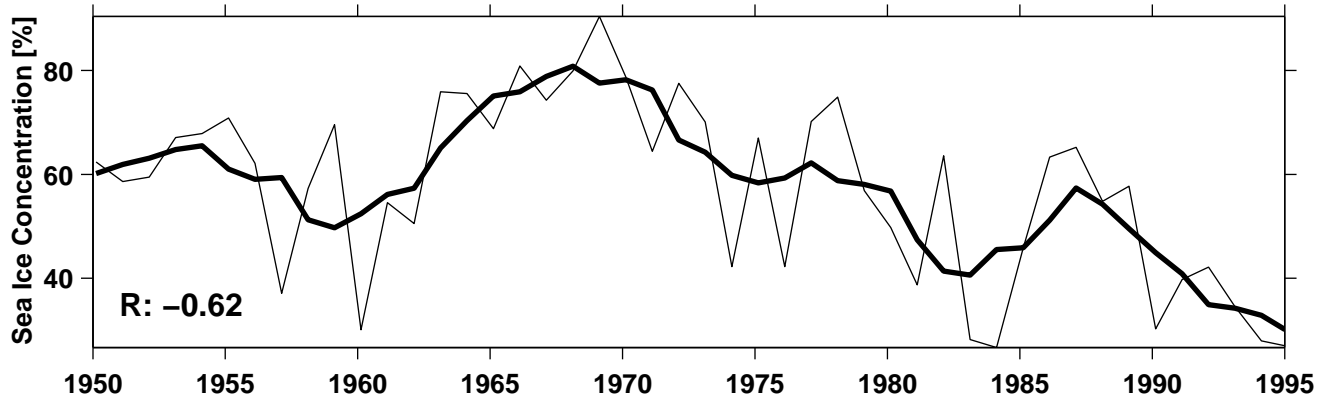




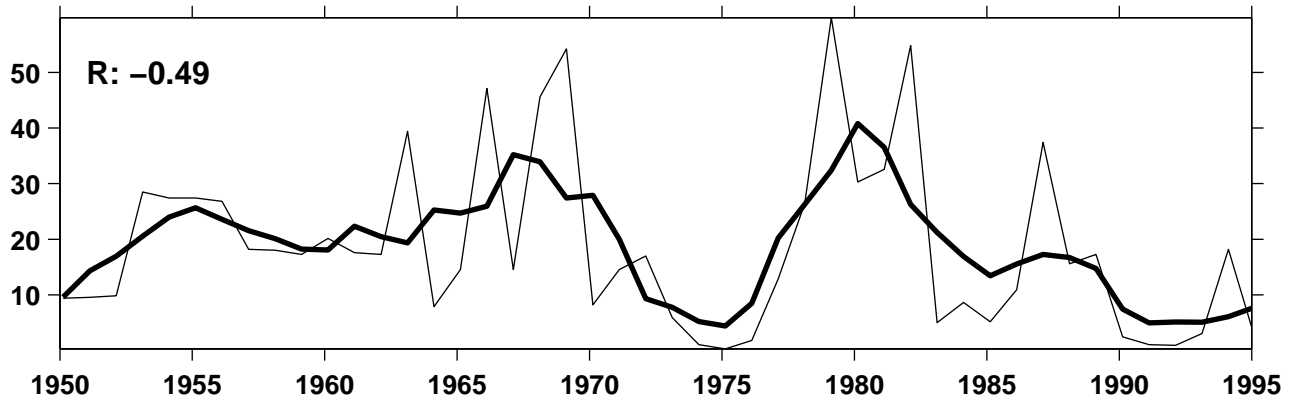
Labrador Sea



Greenland Sea



Barents Sea



NAO index

